



SMR.1065 - 2

# COLLEGE ON SOIL PHYSICS

## 14 - 30 APRIL 1998

---

**"Soil porous systems"**  
**"Saturated and unsaturated hydraulic conductivity"**  
**"Types of preferential flow"**  
**"Elementary hydrologic processes Part I & II"**  
**"Soil sealing and crusting"**  
**"Soil hydrostatics: from parallel tube models to  
fractal fragmentation and percolation models"**  
**"The scale of observation and modeling in soil hydrology Part I & II"**  
**"Evaporation and evapotranspiration"**


**Miroslav KUTILEK**  
**Czech Technical University**  
**Katedra Hydromelioraci**  
**Fakulta Stavebni**  
**Thakurova 7**  
**16629 Prague**  
**CZECH REPUBLIC**

---

**These are preliminary lecture notes, intended only for distribution to participants**

# 1. SOIL POROUS SYSTEMS

---

**SH**  M. Kutilek & D.R. Nielsen: SOIL HYDROLOGY, Catena, 1994

---

**The term pore denotes that part of pore space which is not filled by the soil solid phase.** The shape, size and origin are secondary features and they may play a role only in some detailed classifications.

1. Definition of soil porosity  $P$  and void ratio  $e$ : **SH**, p. 16-20.

Dependence of porosity upon soil water content in swelling soils: **SH**, p. 19.

2. Representative elementary volume, REV: **SH**, p. 16-17.

REV in derivation of Richards' eq.: **SH**, p. 112-114, where  $\Delta x$ ,  $\Delta y$ ,  $\Delta z$  have the size of REV in homogeneous soil with mono-modal pore size distribution.

3. Methods of porosity measurement:

- 3.1. Direct methods. Delesse-Rosinwal principle: **SH**, p. 22-25.

- 3.2. Indirect methods: **SH**, p. 21-22 and Table 3.1., p. 28.

**CAUTION:** Never determine  $P$  just by saturating soil with water,  $P \neq \theta_s$ .

4. Classification of pores: **SH**, p. 20-21.

## **EXTENSION:**

1. Submicroscopic pores, see **SH**, p. 20

2. Micropores or capillary pores. Transport processes in bodies with microporous systems are described by Richards' eq. and by convective-diffusion eq. We distinguish:

- 2.1. Matrix (intrapedal) pores within soil aggregates, their shape, size, coatings of walls, cuttans and nodules depend upon the soil genesis and they are stable in long term time span if no amendments are applied.

- 2.2. Interaggregate (interpedal) pores between the soil aggregates. They are stable in soils which are not affected by intensive agriculture with heavy machinery and high application of fertilizers, and their morphology depends upon the soil genesis. In soils under intensive agriculture their volume and shape are negatively influenced. The boundary between the two categories has to be defined from the analysis of pore size distribution, the equivalent pore radius is with rough approximation between 15 to 30  $\mu\text{m}$ . Interaggregate pores are sometimes misinterpreted as macropores.

3. Macropores, or non-capillary pores of such a size that capillary menisci are not formed across the pore, the shape of air-water interface is planar. The boundary between micropores and macropores is formed by the equivalent pore radius approximately  $r = 1$  to 2 mm. The flow of water inside of these pores is either in the form of a film on the walls of the pore, or filling the whole crosssectional area of the pore, described either by a modified form of the Chézy eq., or by the kinematic wave eq. Origin of macropores is closely correlated to their stability and persistence in time:

- 3.1. Macropores formed by the activity of pedo-edaphon as decayed roots, earthworm channels etc. They have tubular form and they are well persistent in time and relatively independent upon variation of the soil water content. Some channels originated from the hair-roots may belong to the category 2.2 of micropores.
- 3.2. Fissures and cracks occurring as the consequence of volumetric changes of swelling-shrinking soils. They have planar forms and they are dependent upon the soil water content, at their high values they gradually disappear.
- 3.3. Macropores originating due to the soil tillage. Their depth is limited, they are dependent upon soil water content and disappear usually in less than one vegetation season, the persistence depends upon meteorological situations and type of plants.

Soil porous system with 2.1. plus 2.2. is sometimes denoted as system with dual porosity. In some instance soils with micropores and macropores are denoted as soils with dual porosity. The terminology is not unified. The same is for the quantitative characteristic of macropores.

5. Estimation of the soil porous system: **SH**, p.22-25.

Soil water retention curve (SWRC) is the summation curve. Its derivative curve with  $r$  replacing pressure head  $h$  is the pore size distribution curve (PSD). One inflection point on SWRC means one peak on PSD and pore size distribution is mono-modal, Fig. 1.1 For 3 inflection points on SWRC we get bi-modal PSD, there is evidence on at least tri-modal PSD in some soils with a well developed aggregation (primary, secondary, tertiary peds). The mutual arrangement is hierarchical, SWRC is deconstructed on the principal of inversion of superposition, Figs. 1.2. to 1.5.

6. Alteration of the soil porous system:

6.1 With soil water content: **Vertisols**, see **SH**, Fig. 2.3., p. 19 and the text and **SH**, Fig. 4.24, p. 84 and the text.

**EXTENSION** on cracks in Vertisols of arid zone (A) and of mild zone (M):

Mean width of cracks on the topographical surface (TS) is 3.5 cm (A), 0.3 cm (M),

Distance between cracks on TS is 20-50 cm (A), 20-100 cm (M),

Length of cracks per area 2.8 cm/cm<sup>2</sup> (A).

Depth of cracks 40-80 cm (A), 40-100 cm (M)

Crack porosity 2.5 % - 5% (A), 1 % - 9%, average 4% (M) if dry.  
(Kutilek, 1996).

6.2 Role of intensive agriculture: Soil compaction leads to irreversible destruction of interaggregate pores, especially below the plough horizon, n-modal soil pore distribution is gradually changed to nearly monomodal.

6.3 Role of soil amendments and of soil conditioners: The whole pore size distribution system should be studied, see e.g. Pagliai and Viozzzi (1998), Fig. 1.6

6.4 Time scale in alteration of porous system, Fig. 1.7.

**Additional references:**

- Kutilek, M., 1996. Water relations and water management of Vertisols. In: N. Ahmad and A. Mermut (Eds.): Vertisols and Technologies for their Management. Elsevier, p. 201-230.
- Pagliai, M. and N. Viozzzi, 1998. Use of manures for soil improvement. In: A. Wallace and R.E. Terry (Eds.): Handbook of Soil Conditioners. Marcel Dekker, p. 119-139.

RECENT ASSUMPTION —  
— MICROMORPHOLOGICAL  
HOMOGENEITY (III) & FREE ACCESS  
(II)

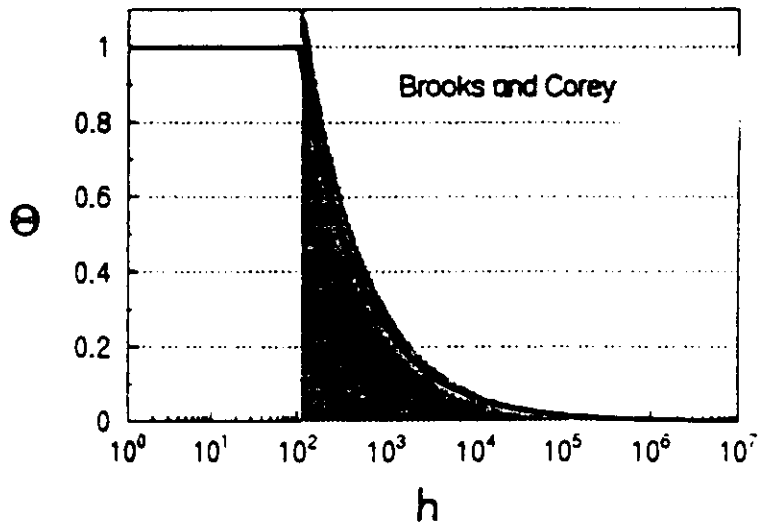
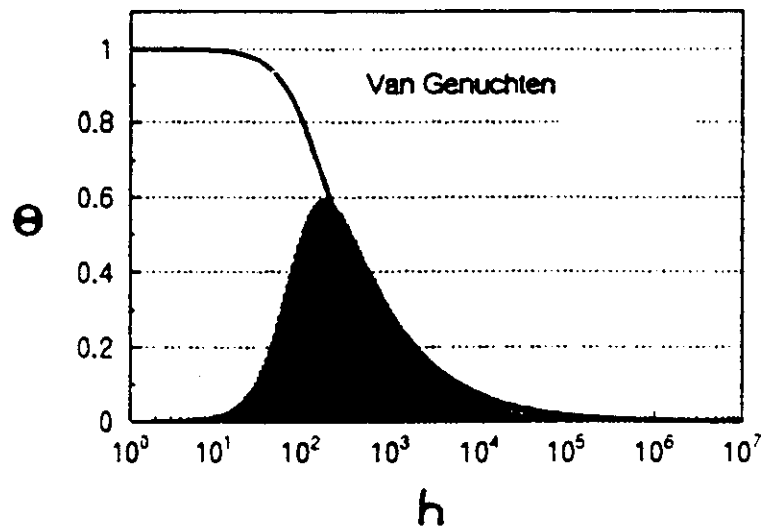


FIG 1.1

DUE TO EXISTENCE OF PEDS &  
CUTANS (= COATING OF PEDS)

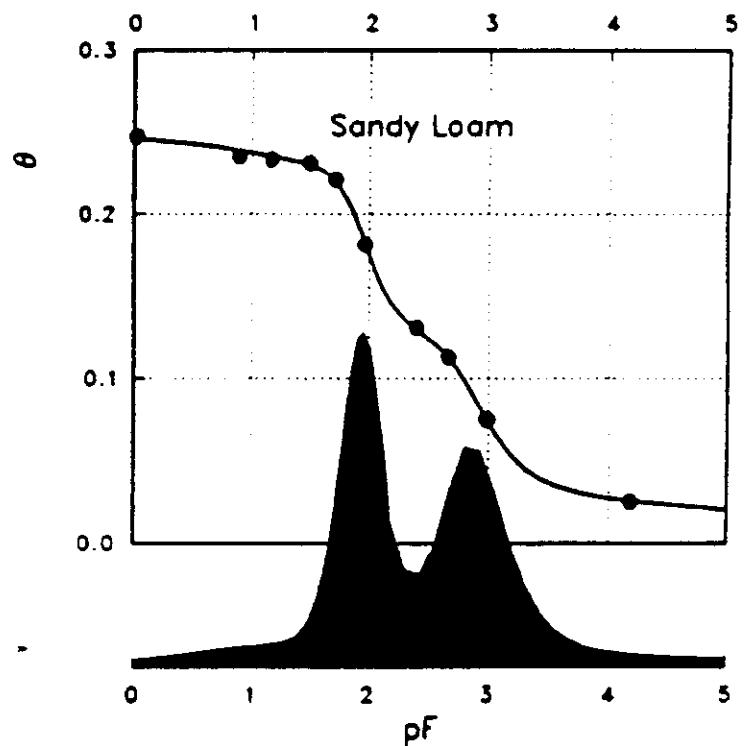
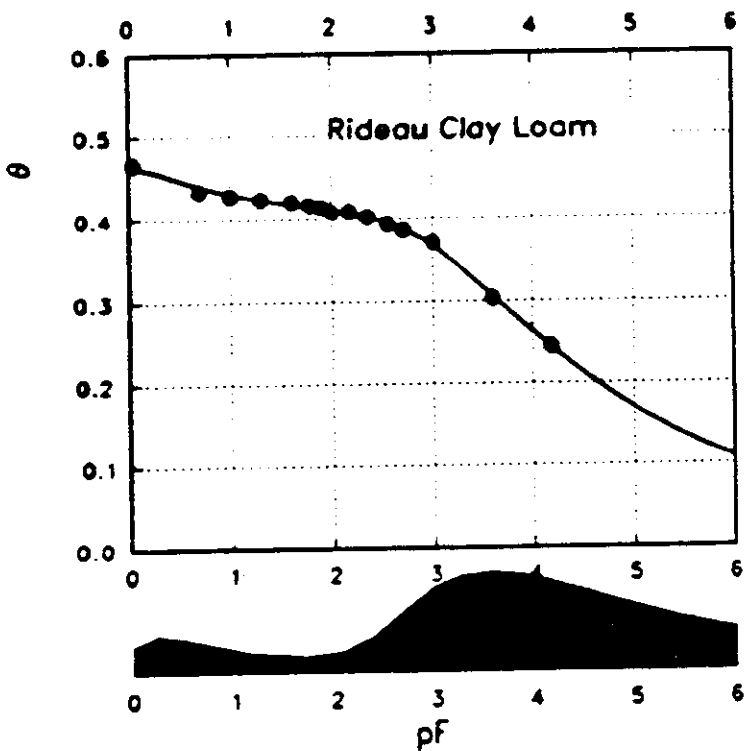
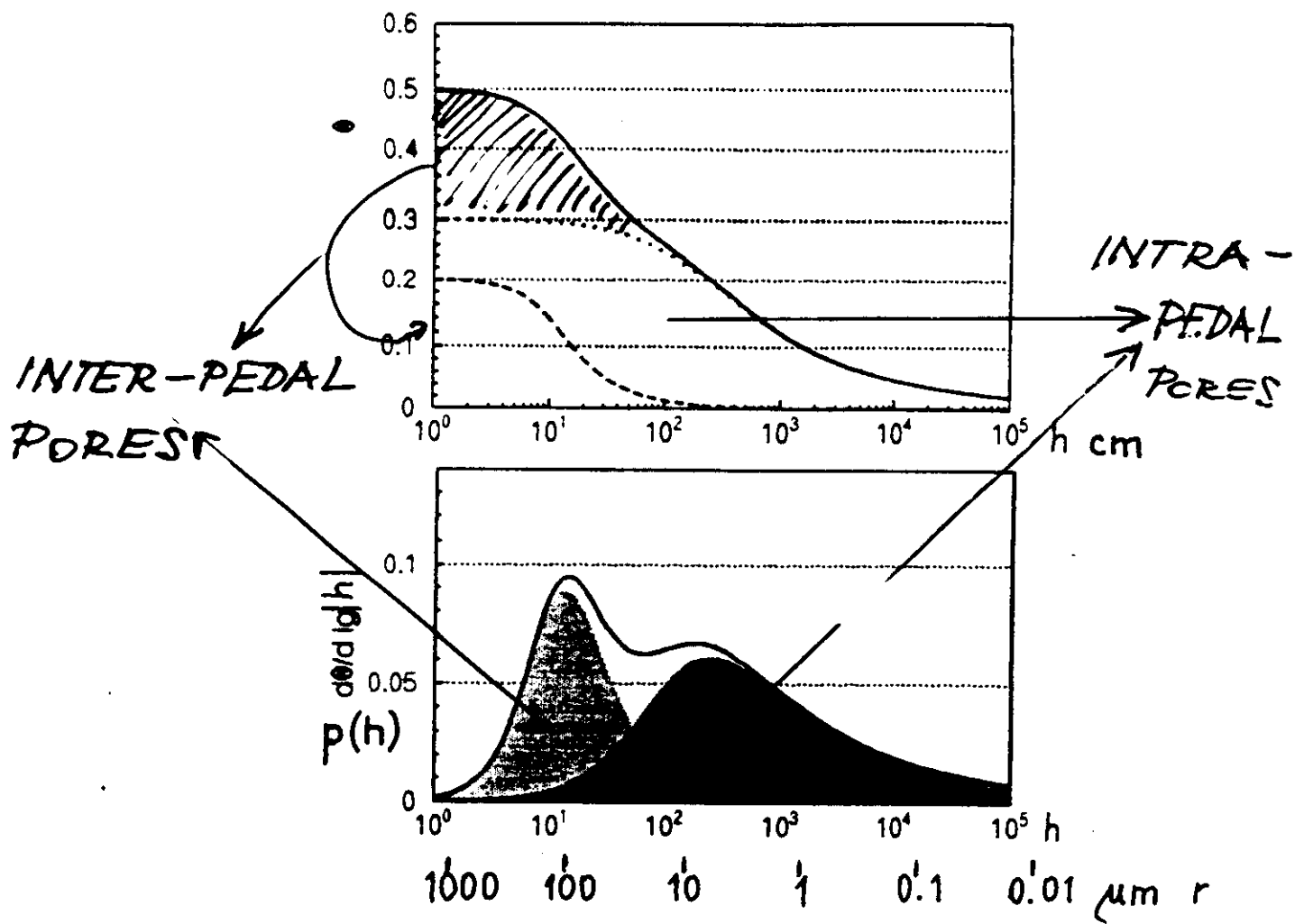


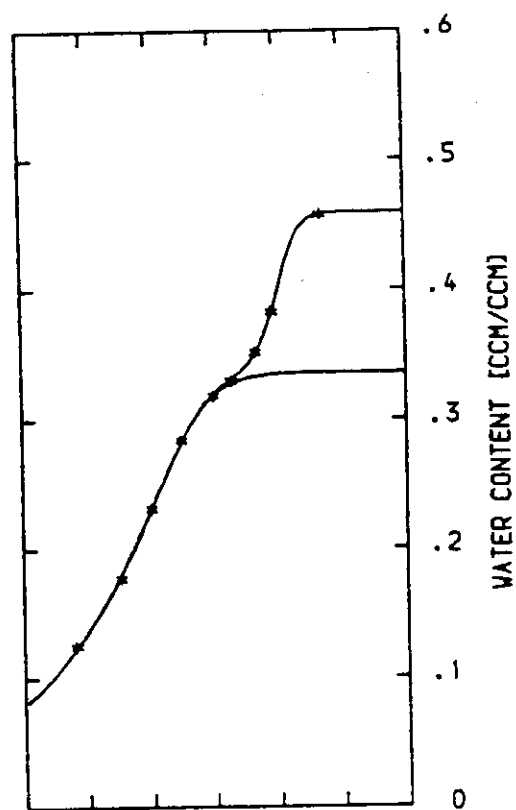
FIG 10

# A-HOR. CAMBISOL ON LOESS 31-MODAL SWRC

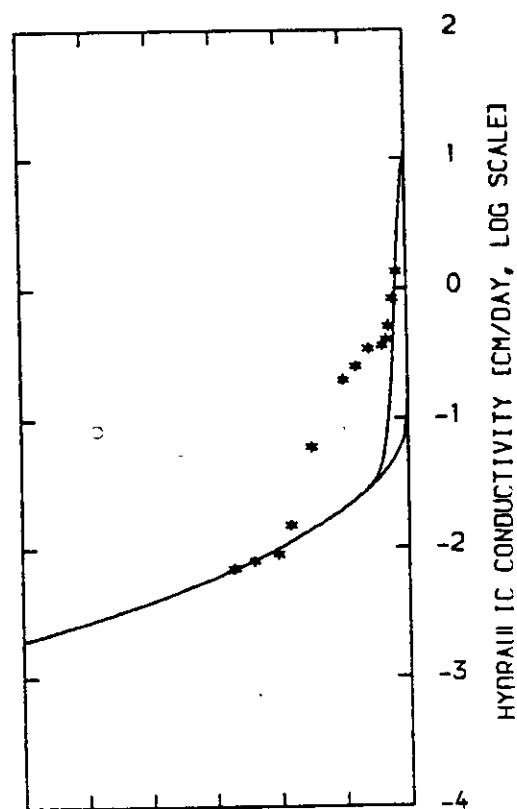
LEITZ 4734  
 Made in West Germany

LOAM, DEPTH: 15CM

\*\*\* MEASUREMENTS



5 4 3 2 1 0 -1  
 SUCTION HEAD [HPA, LOG SCALE]



-300 -250 -200 -150 -100 -50 0  
 MATRIC POTENTIAL [HPA]

PARAMETER:

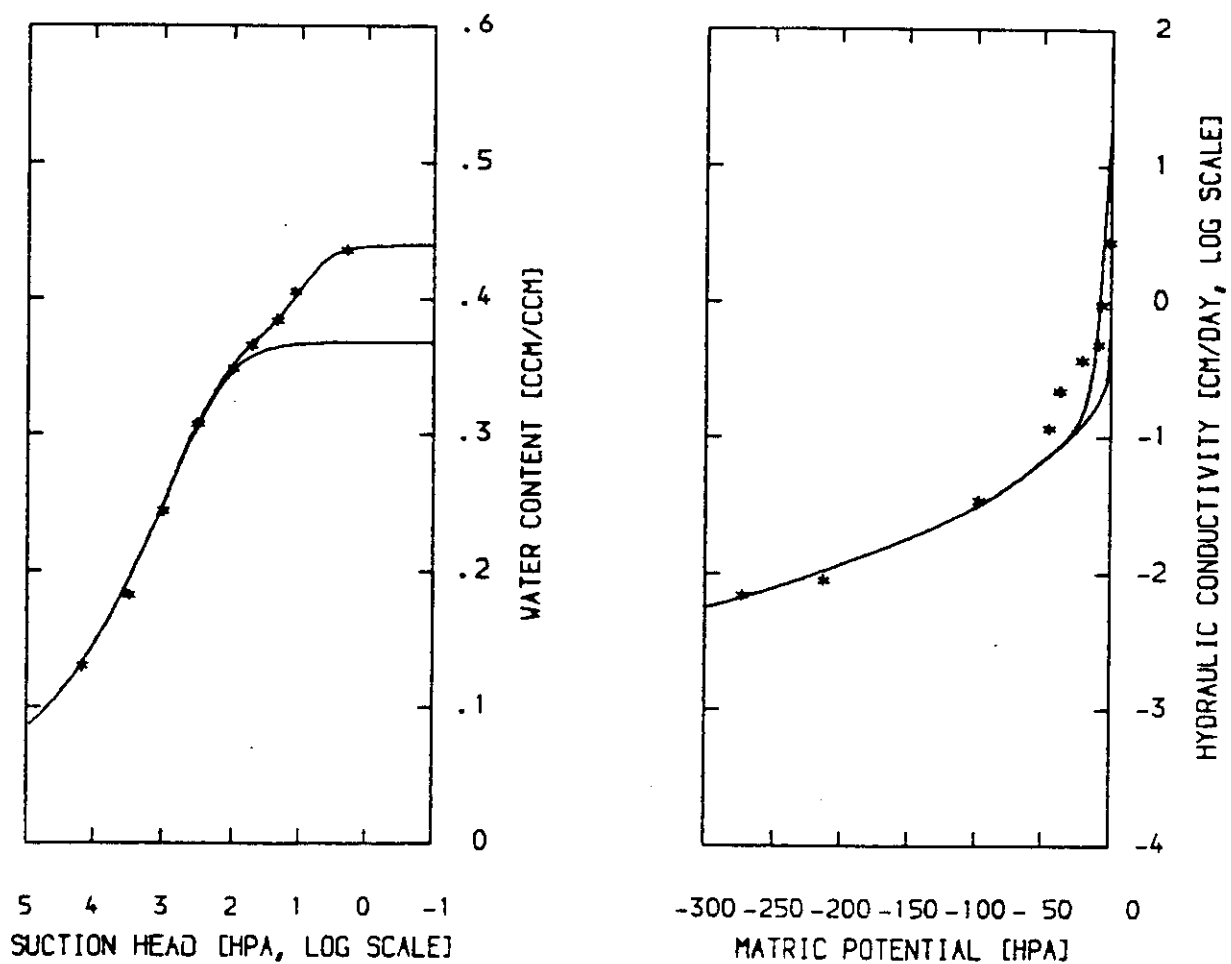
PORE SYSTEM 1: THETAS: 33.60 THETAR: 1.38 KS: 0.15 ALPHA: 0.0039 N: 1.2  
 PORE SYSTEM 2: THETAS: 12.36 THETAR: 0.00 KS: 11.50 ALPHA: 0.1262 N: 2.9

FIG. 1.3.

# A-B HOR. CAMBISOL ON LOESS

LOAM, DEPTH: 30CM

\*\*\* MEASUREMENTS



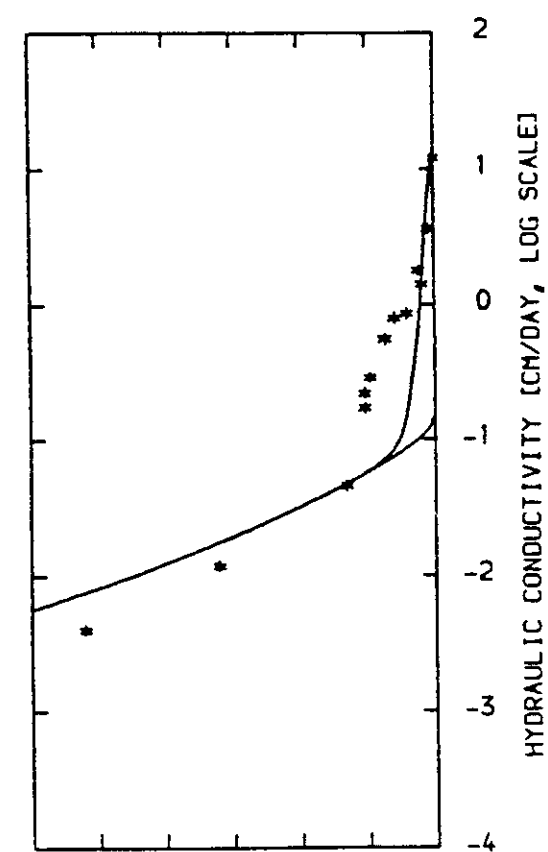
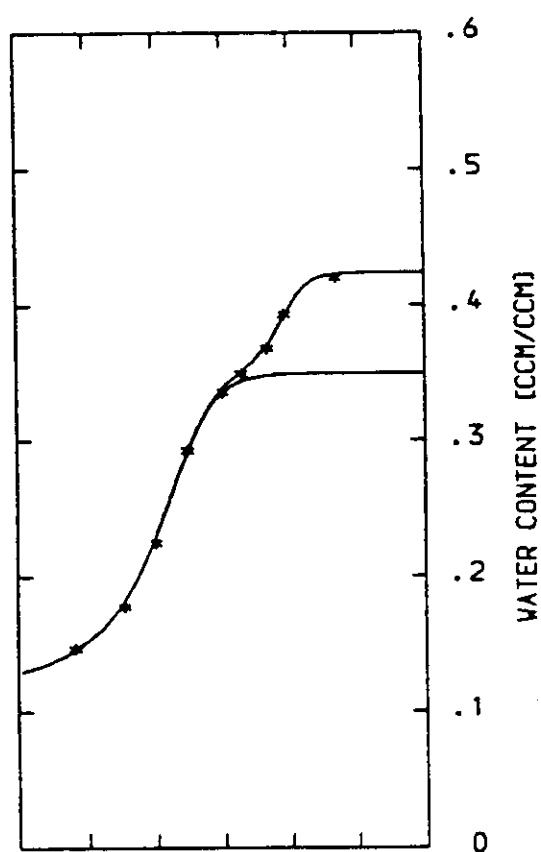
PARAMETER:  
 PORE SYSTEM 1, THETAS, 36.87 THETAR, 0.50 KS, 0.60 ALPHA, 0.0044 N, 1.25  
 PORE SYSTEM 2, THETAS, 7.10 THETAR, 0.00 KS, 19.76 ALPHA, 0.1500 N, 2.00

FIG. 1.4

B-HORIZON CAMBISOL  
POLYEDER STRUCTURE  
B1-MODAL

LOAM, DEPTH: 60CM

\*\*\* MEASUREMENTS



PARAMETER:  
SUCTION HEAD [HPA, LOG SCALE]

MATRIC POTENTIAL [HPA]

PARAMETER:

PORE SYSTEM 1: THETAS: 34.87 THETAR: 12.00 KS: 0.15 ALPHA: 0.0035 N: 1.55  
PORE SYSTEM 2: THETAS: 7.50 THETAR: 0.00 KS: 15.00 ALPHA: 0.1000 N: 2.40

FIG. 1.5



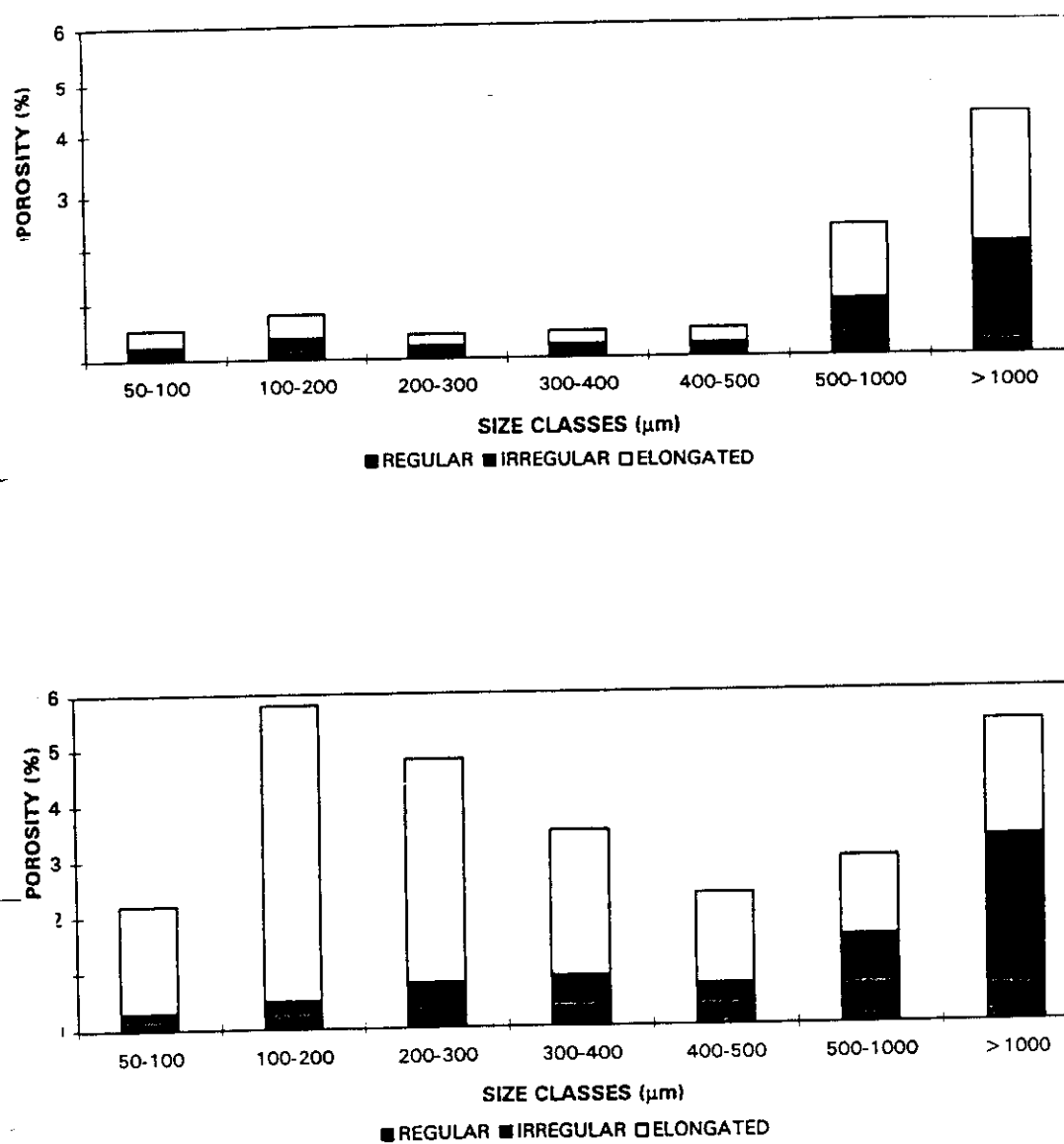
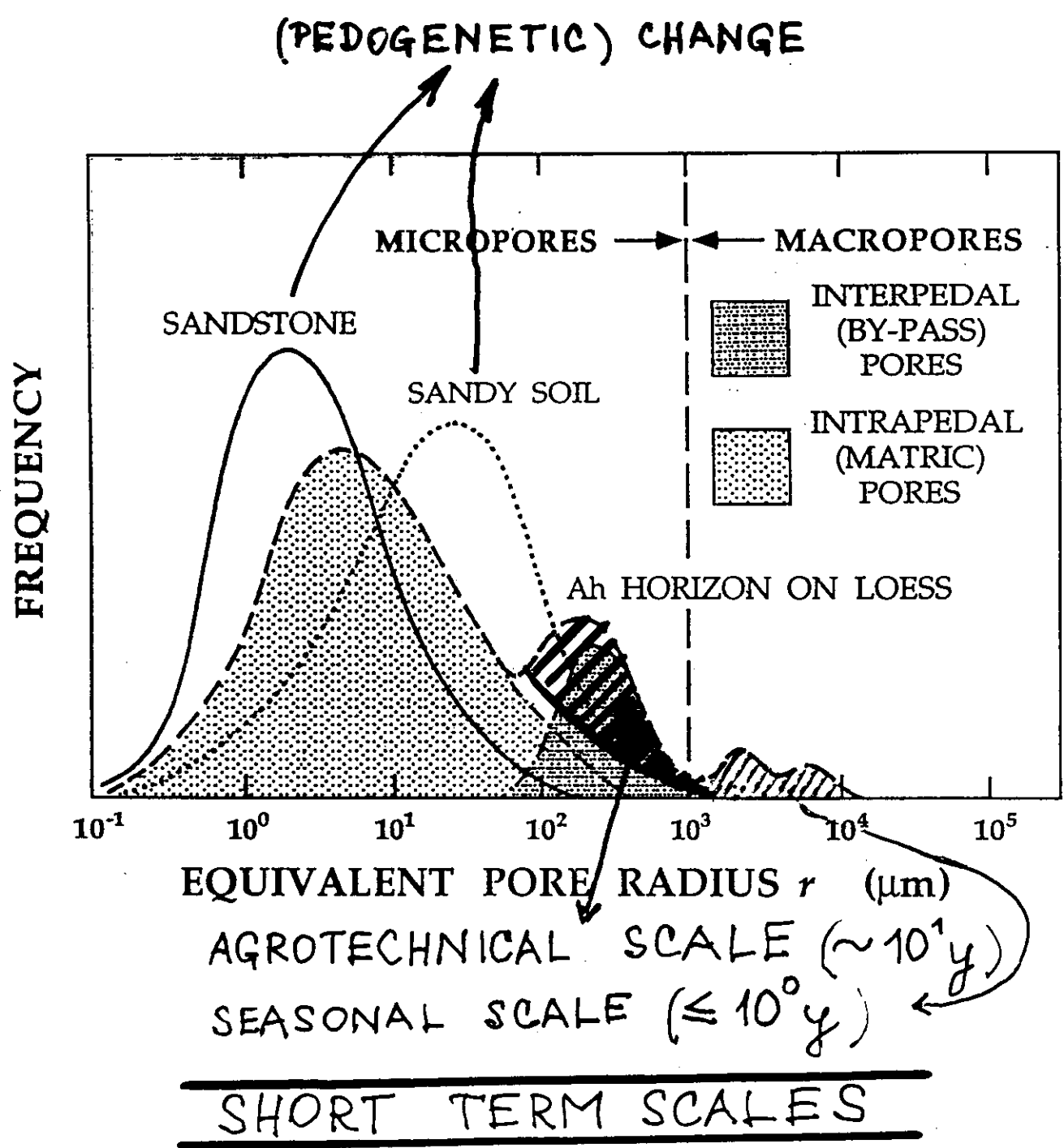


**Figure 5** Pore size distribution of pores larger than 50  $\mu\text{m}$ , determined by image analysis on thin section according to the equivalent pore diameter for regular and irregular pores and width for elongated pores, in control plots of the same silty clay soil of Fig. 2 and in plots treated with 300  $\text{MG ha}^{-1}$  of pig slurry applied at the end of May. (Modified from Pagliai and Vittori Antisari, 1993.)

FIG. 1.6

LONG TERM SCALE ( $> 10^2$  y.)  
(PEDOGENETIC SCALE)



**TIME SCALES**

FIG 1.3

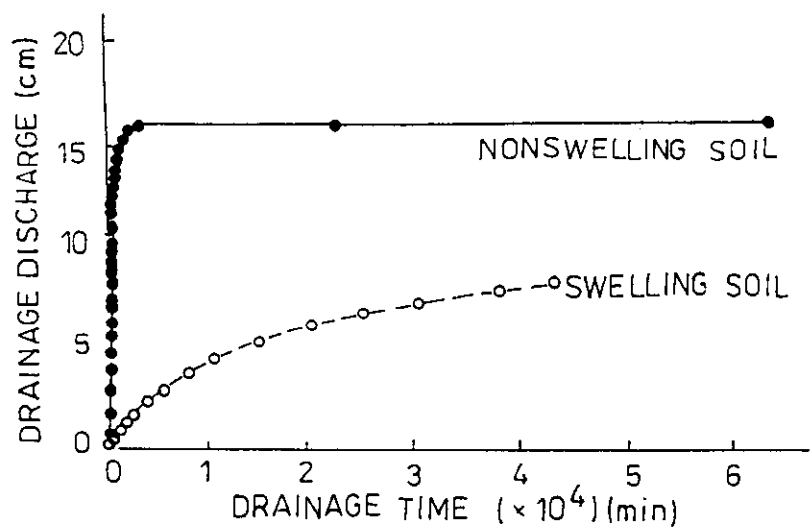


FIG. 1.7

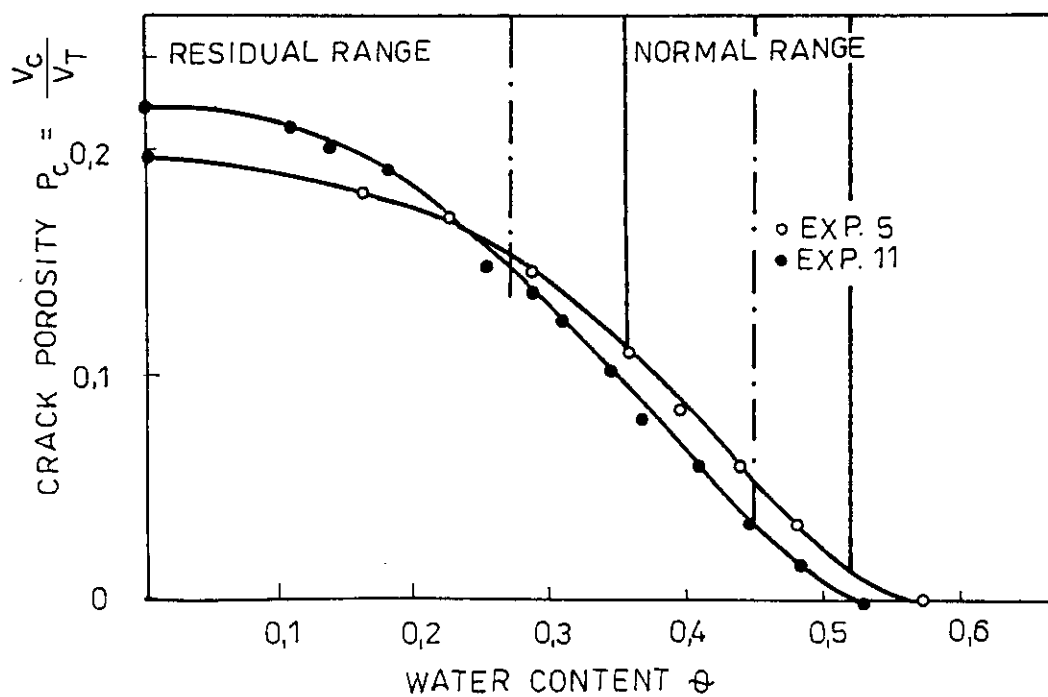


FIG. 1.8

## 2. SATURATED AND UNSATURATED HYDRAULIC CONDUCTIVITY

---

**SH** M. Kutilek & D.R. Nielsen: SOIL HYDROLOGY, Catena, 1994

---

1. Flow in porous media: **SH**, p. 87-88.
2. Saturated flow: Darcy's eq.: **SH**, p. 88-91.
  - 2.1. Saturated hydraulic conductivity, Kozeny's model and eq.: **SH**, p. 91-94, 96.
  - 2.2. Alteration of hydraulic conductivity due to:
    - 2.2.1. Clogging of pores: **SH**, p. 94 and Fig. 5.10 on p. 107.
    - 2.2.2. Salinity and alkalinity: **SH**, p. 94-96.
  - 2.3. Measuring of saturated hydraulic conductivity: **SH**, p. 98-101.
3. Unsaturated flow: Darcy-Buckingham eq.: **SH**, p. 102-104.
 

Unsteady flow, Richards' eq.: **SH**, p. 112-116.

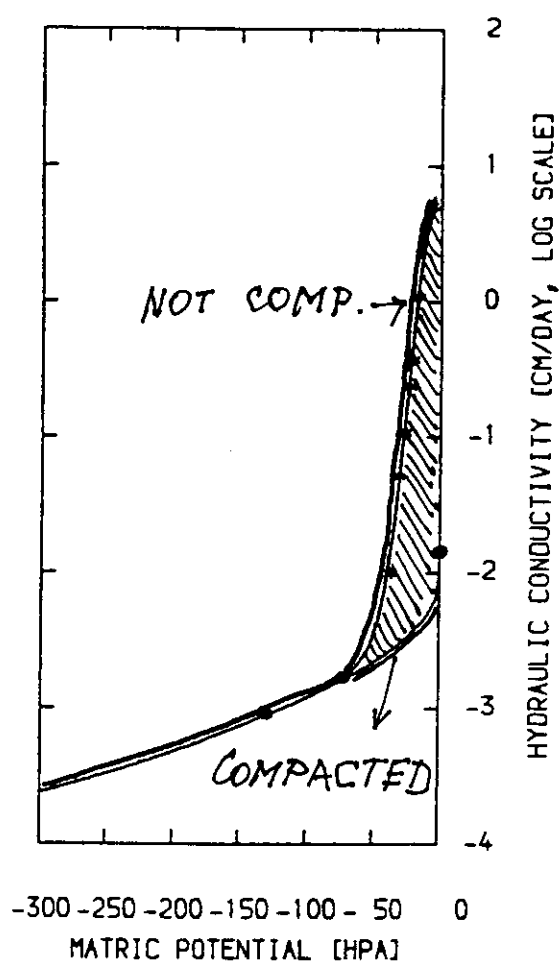
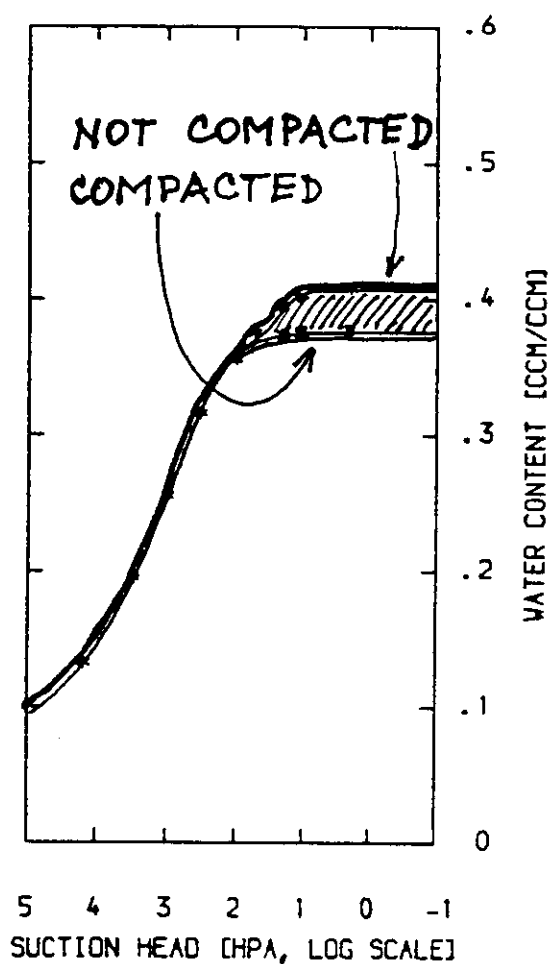
  - 3.1. Unsaturated hydraulic conductivity: **SH**, p. 104-106.
  - 3.2. Its capillary model: **SH**, p. 106-110.
  - 3.3. Unsaturated hydraulic conductivity in soils of bi-modal porous system: **SH**, p. 110-111. Fig. 1.3 to 1.5.
  - 3.4. Soil compaction and unsaturated hydraulic conductivity, Fig. 2.1.
  - 3.5. Soil alkalinity and soil water diffusivity, **SH**, p. 116-117.
4. The above derived equations are valid for flow in rigid soils. For information on flow in swelling-shrinking soils see introduction on transformation to Lagrangian coordinates **SH**, p. 123-124. Flow in deformable soils with three-dimensional volumetric change when flow in cracks is not considered is described by Garnier et al. (1997). The hydraulic characteristics  $h(\theta)$  and  $K(\theta)$  and the deformation curve  $e(\theta)$  could be estimated by inverse method from the evaporation experiment where the horizontal and vertical deformations are measured on core samples,  $e$  is void ratio,  $\theta$  is soil water ratio.

### Additional reference:

Garnier, P., M. Rieu, P. Boivin, M. Vauclin and P. Baveye, 1997. Determining the hydraulic properties of a swelling soil from a transient evaporation experiment. Soil Sci. Soc. Am. J. 61:1555-1563.

COLLUVIUM, DEPTH: 25CM

\*\*\* MEASUREMENTS



PARAMETER:


PORE SYSTEM 1: THETAS: 37.60 THETAR: 5.00 KS: 0.01 ALPHA: 0.0034 N: 1.35

PORE SYSTEM 2: THETAS: 3.10 THETAR: 0.00 KS: 5.00 ALPHA: 0.0500 N: 3.50

FIG. 2.1

### 3. TYPES OF PREFERENTIAL FLOW

---

**SH**  M. Kutilek & D.R. Nielsen: SOIL HYDROLOGY, Catena, 1994

---

Three types of preferential flow:

1. In soil porous system due to soil micro- and macro-morphology.
2. Fingering mainly due to instability on the wetting front..
3. Irregularities in hydrophility.

1.1. Preferential flow in interaggregate (interpedal) pores, i.e. category of soil pores 2.2.: If saturated hydraulic conductivity of matrix is  $K_s = 1$ , then matrix plus interaggregate  $K_s = 10^2$ , unsaturated flow in matrix is negligible in the first approximation. See **SH**, Fig. 5.12, p. 111. This type of preferential flow is sometimes misinterpreted as flow in macropores.

**EXTENSION:** See Figs. 1.3 to 1.5. Preferential flow plays a significant role in A, B horizons. The role of preferential flow upon modeling of soil water regime, Fig. 3.1.

1.2. Preferential flow in macropores, i.e. Category 3.  $K_s$  is by one order or more greater than in saturated micropores. ~~Flow in cracks reaches to the depth 100 cm maximum.~~ Flow in cracks reaches to the depth 100 cm maximum. In biopores it reaches usually below the pedogenetic depth.

Partial review of the problem is in a serie of papers of Ju et al. (1997). However, there is a mess in terminology and definitions. It is frequent that the flow in category 2.2 of pores is denoted as flow of mobile water, while the solution in the category 2.1. is named immobile water. Flow in 2.2 is named funnel flow, too.

#### IMPLICATIONS IN MEASURING TECHNIQS OF THE TRANSPORT OF POLLUTANTS

The heterogeneous soil porous system plays a dominant role upon what we are actually measuring when we are dealing with the transport of pollutants in the field.

Soil sampling and the next laboratory determination of the content of pollutants offers information on the solution in micropores, only. When the core samples are taken without deforming them, solution in the whole system of category 2.1. is determined while in the category 2.2. the unknown portion is taken and determined since the size of the core sample is usually less than REV. Even high number of samples can not guarantee a representative result when the same weight is given to each sample in statistical evaluation and when the space variability is neglected. When the samples are taken by augers, they are usually more or less compressed and the solution from 2.2 is lost unless some special technics is developed to avoid pressure on walls of cores, Fig. 3.3

Gravity lysimeters are provided by the impervious plate on the bottom of the undisturbed part of the soil profile. Flux of the solution through macropores is collected and even a part of solution in 2.2 pores may contribute to it in the wet season. The criterion on REV is usually reached. Similar results are obtained when the solution is collected by tile drains provided that the backfill is protected form the application of the chemical on the topographical surface.

Even old backfills have different porous systems and flux characteristics from the surrounding soil, Fig. 3.4. *a, b, c*.

Suction lysimeters are provided by a porous plate at the bottom and via the applied negative pressure the solution is collected from all pores of category 3 and from the part of 2.2. This portion is limited in its equivalent diameter by the applied suction at the bottom plate. If this suction is at least -100 hPa, we can assume that practically all preferential pores are drained and the solution represents the preferential flow if the criterion on REV is reached, Fig. 3.5.

Lysimeters refilled with disturbed soil offer not reliable information on transports in natural soils and we can consider the refilling material as a surrogate soil.

Suction cups collect the solution from pores 2.2 up to equivalent diameter given by the applied negative pressure. There is a low probability of detecting macropores, category 3. Since in majority of instances REV is in size bigger than the domain from which the solution is collected by the cup, a certain number of cups is needed at each depth in order to gain reliable data. The number of cups needed to gain representative data depends upon the size of cups, required accuracy and the soil type. The installation of cups should not disturb the natural soil porous system around the cups, Fig. 3.6.

Resistance blocks offer information on concentration of solution inside of pores 2.1 plus 2.2. Their disadvantage is a long time interval required to reach equilibrium between the solution in porous material of the block and in surrounding soil porous system. The rapid change of concentration in time and space is not detectable. The flow net is not disturbed. Disadvantage related to small size of the block is analogic to suction cups, Fig. 3.7.

TDR offers information on the concentration of the solution in pores 2.1. and 2.2., while macropores are reached rarely. The length of rods is usually sufficient to cover the horizontal length of REV, Fig. 3.8.

## 2. Preferential flow due to fingering: SH, p. 172

A wide variety of instabilities may occur when transport of miscible and immiscible fluids are realized in porous media. Most frequently, they are driven either by viscous and gravity forces. Gravity driven instabilities are related to infiltration and redistribution of water in soil. The linear stability analysis suggests that the water-air interface will be unstable if its velocity is less than the saturated conductivity of the medium. This wetting front instability results in formation of fingers where the transport of water (and solutions) is realized.

The hydrodynamic instability of flow in unsaturated soil may take place due to the soil stratification and the imposed initial and boundary conditions. It is observed when hydraulic conductivity increases with depth and the fluid meets an interface of great variation of  $K$  i.e. from a smaller value (fine texture soil, or compacted upper layer) to a greater value (coarse texture soil, or loose sublayer). The Richards' eq. which usually describes the transport of water, or convective-diffusive equation for transport of solutes assume the validity of the hypothesis on wetting front stability. As this condition is not met, the mentioned equations are not applicable. Due to the instability of the front, narrow zones, „fingers“ of nearly saturation, or of increased water content are formed ahead of the wetting front and these fingers are protruded in time. They occur not only during infiltration, but they have been observed in redistribution, too. Fingers are domains of preferential flow and preferential transport of chemicals in soils. Studies on fingering have been carried out through visual observations, light transmission, image processing and magnetic resonance imaging, see Onody et al. (1995), Fig. 3.9.

Parameters of fingers, as  $d_F$  - finger diameter,  $q_F$  - average flux in the finger are dependent upon  $K_S$ , sorptivity  $S$ , and  $\theta_S$ ,  $\theta_i$ , saturated and initial soil water content.

Theory of fingering is related to the geometry of porous media. With fractal characterization of fingering two type of models were created: Diffusion limited aggregation and Invasion percolation model, for quotation see Onody et al. (1995).

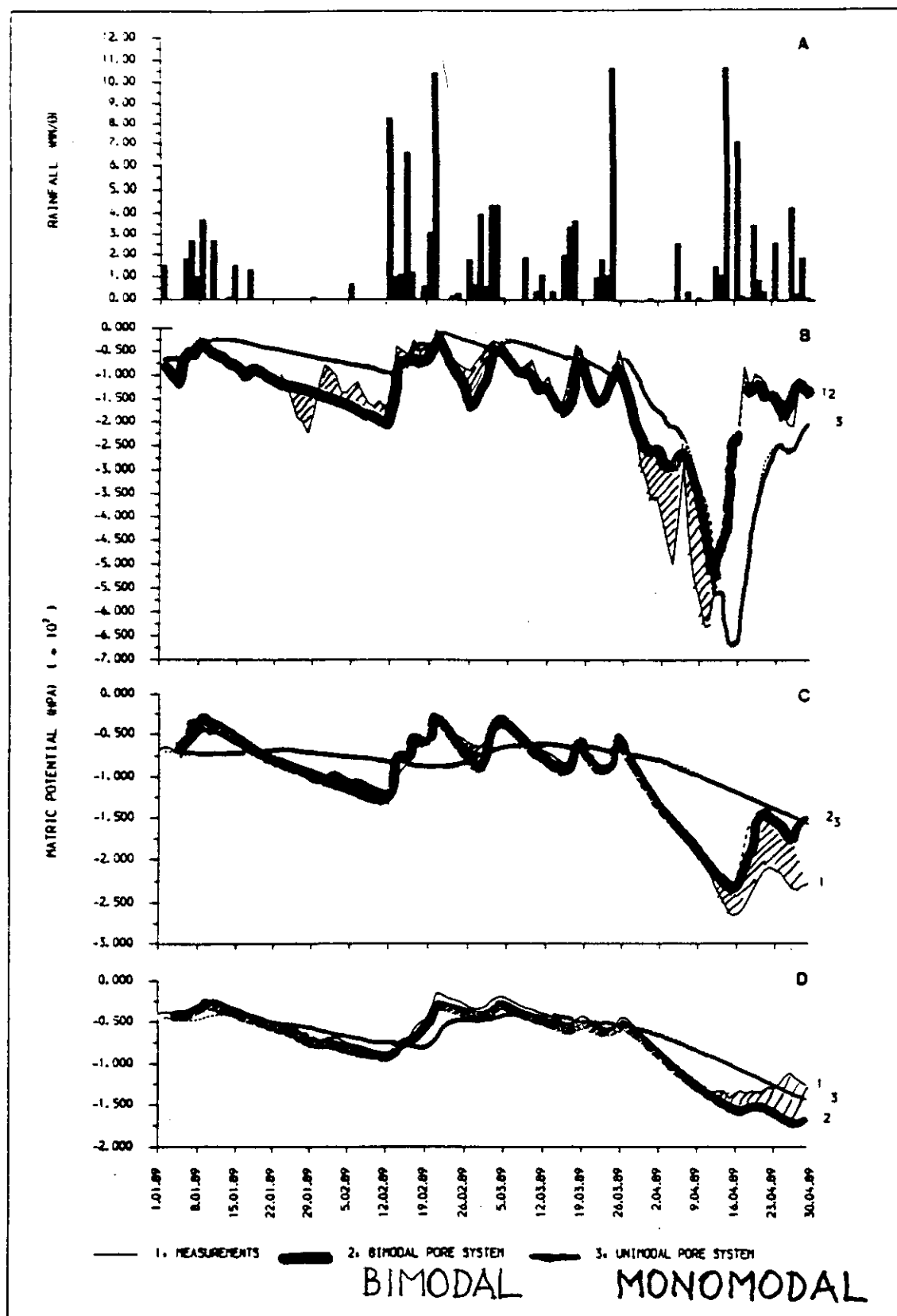
### 3. Irregularities in hydrophility

Dry soil of high organic content and peats are known to inhibit water infiltration, ultimately forcing water to flow via preferential paths through unsaturated vadose zone. Important is the value of critical soil water content  $\theta_{CR}$ . If actual  $\theta < \theta_{CR}$ , the soil behaves as water repellent, i.e. hydrophobic with high value of the wetting angle above  $90^\circ$ . With water-entry value of the boundary wetting branch beneath the air entry value of the main drainage branch, perturbations occur leading to formation of fingers, Fig. 3.10. (Ritsema and Dekker, 1994, Ritsema, 1998). The observed fingering was up to now restricted to sandy soils with high organic matter content.

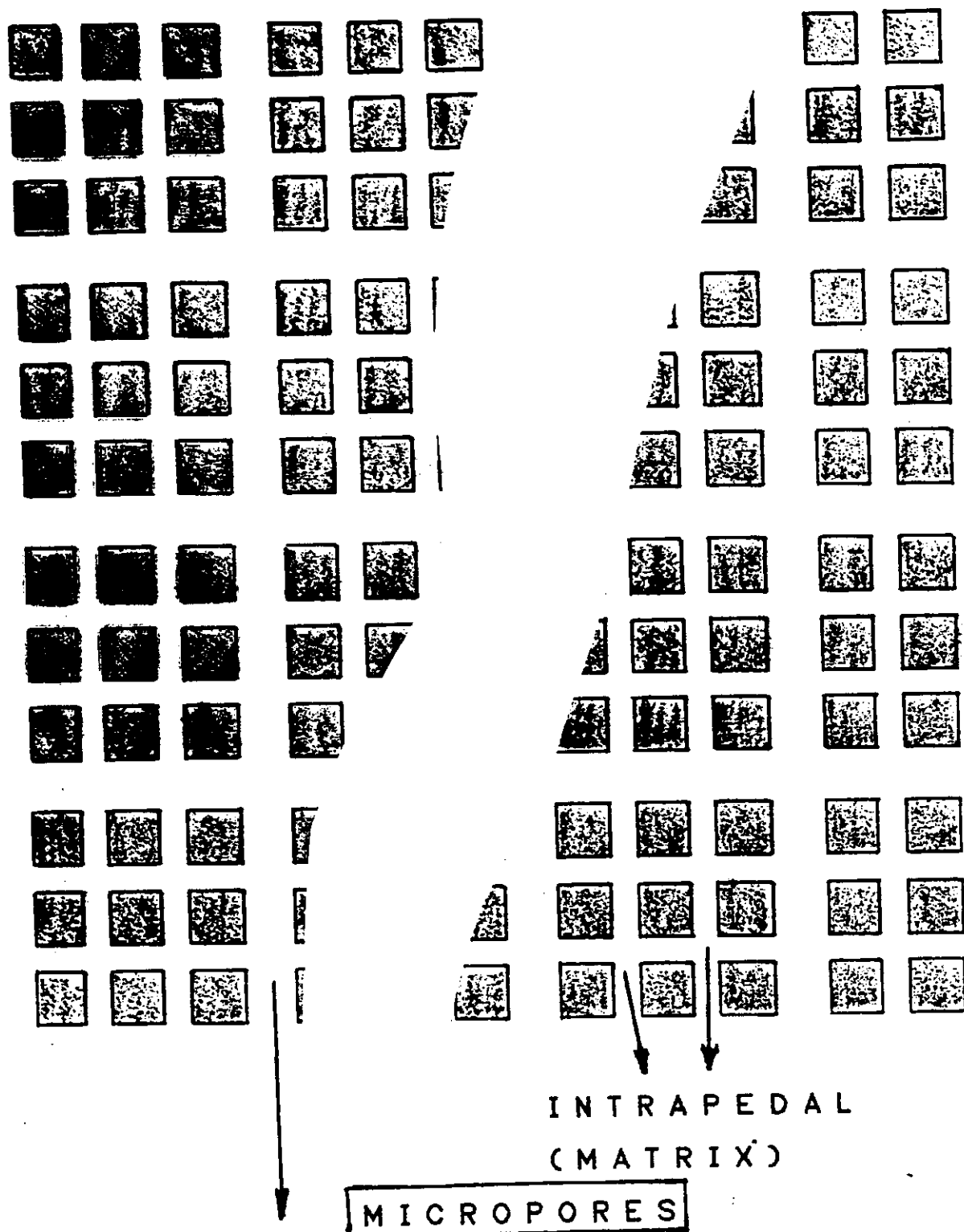
### Additional references:

- Ju, S.-H. and K.-J.S. Kung. 1997. Impact of funnel flow on contaminant transport in sandy soils. *Soil Sci. Soc. Am. J.* 61:409-415 and also: 61:416-427, 61:427-435.
- Kutilek, M., 1997. Measurements of environmental parameters. In: P.E. Cruvinel, S. Crestana, L.M. Neto, L.A. Colnago, and L.H.C. Mattoso: *Anais do I Siagro I Simpósio Nacional de Instrumentação Agropecuária*. EMBRAPA-CNPDI, pp.43-49.
- Onody, R.N., A.N.D. Posadas, and S. Crestana, 1995. Experimental studies of the fingering phenomena in two dimensions and simulation using a modified invasion percolation model. *J. Appl. Phys.* 78:2970-2976.
- Ritsema, C.J. and L.W. Dekker, 1994. How water moves in a water repellent sandy soil. 2. Dynamics of fingered flow. *Water Resour. Res.* 30:2519-2531.
- Ritsema, C.J., 1998. Stable or unstable wetting fronts in water repellent soils - Effect of antecedent soil moisture content. *Soil Technology*, in press.





# MACROPORE



INTRAPEDAL  
(MATRIX)

MICROPORES

INTERPEDAL  
(INTERAGGREGATE)

FIG. 3.2

# SOIL SAMPLING

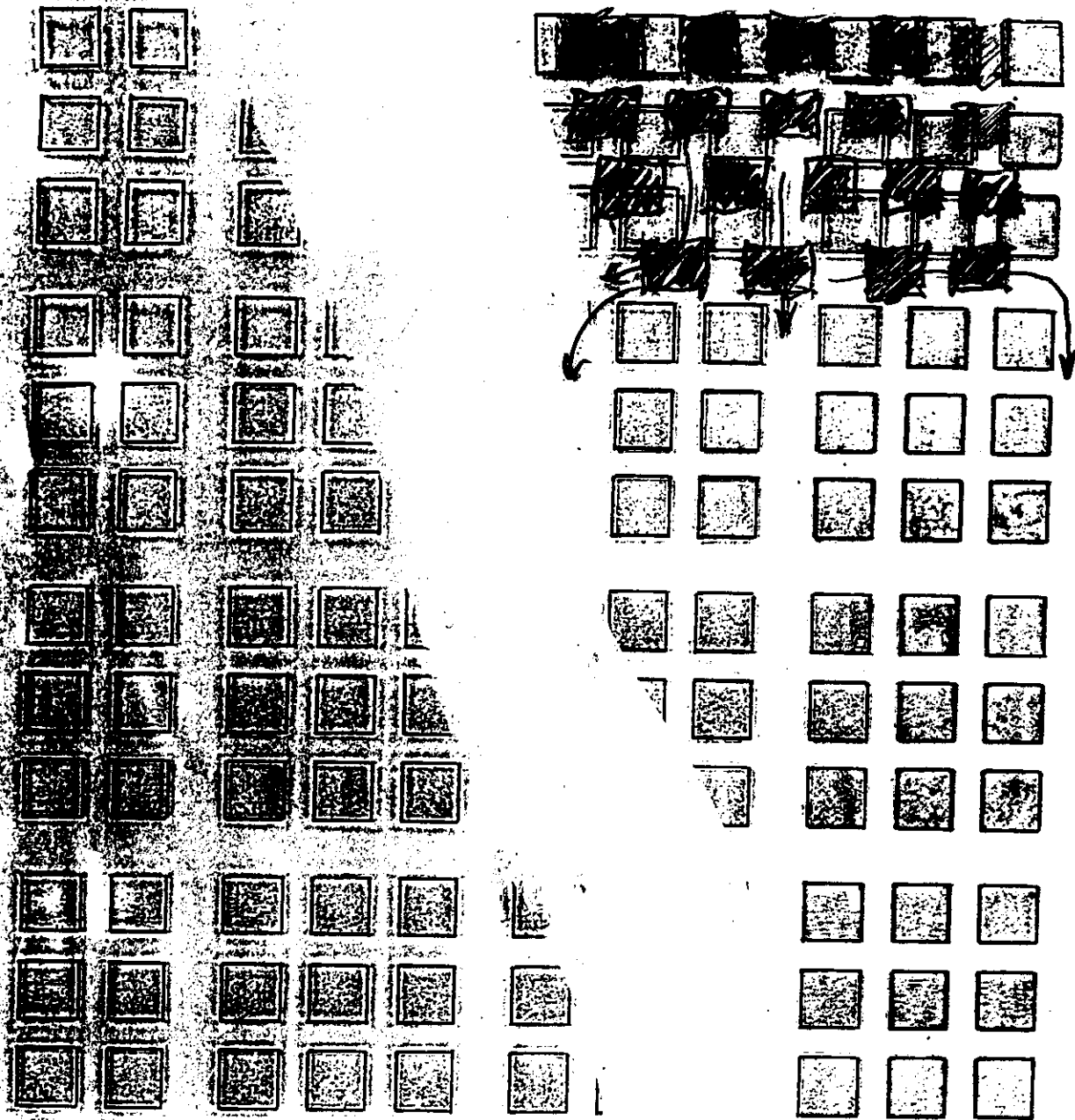
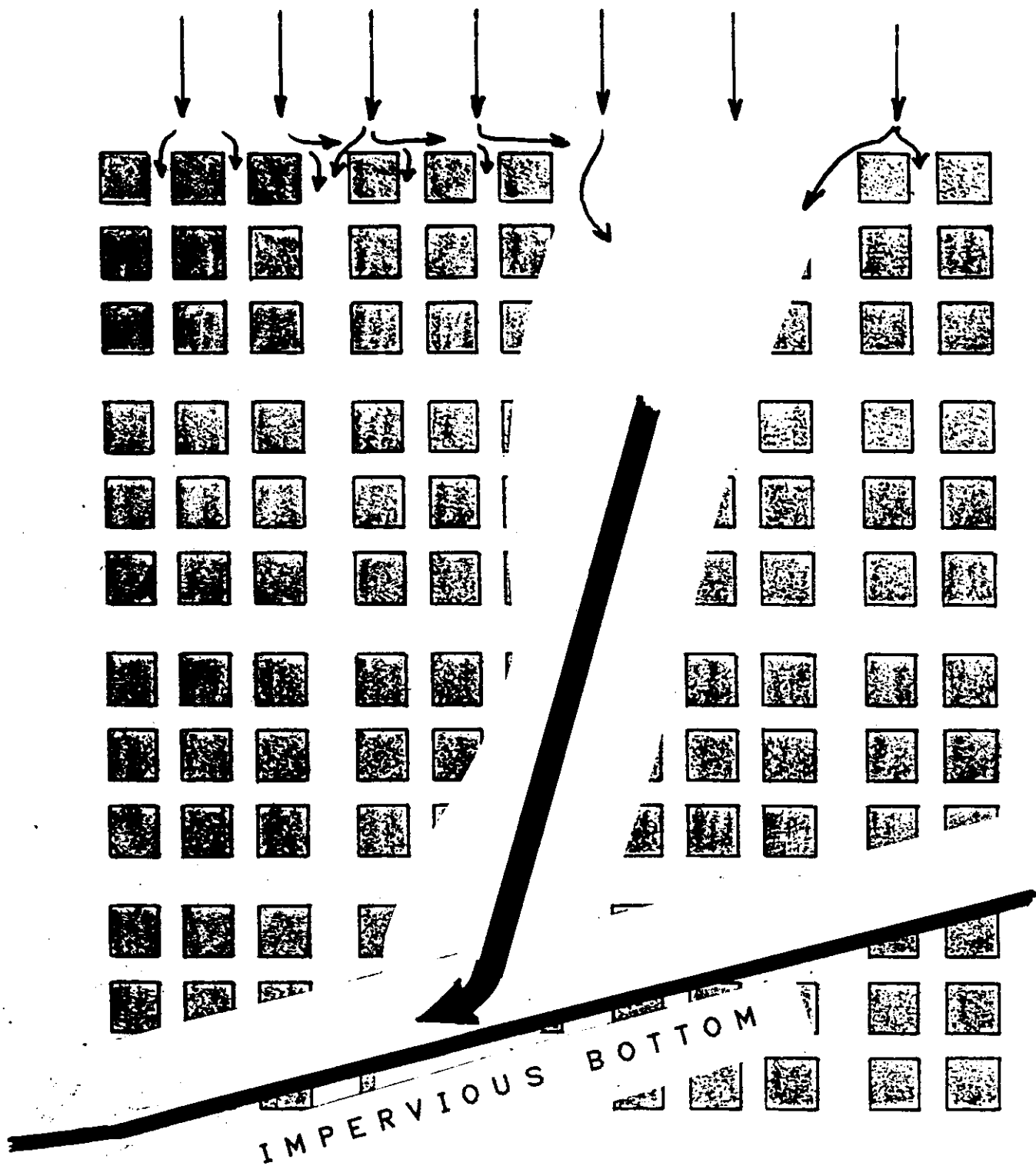


FIG. 3.3



GRAVITY LYSIMETER

FIG. 3.4.a)

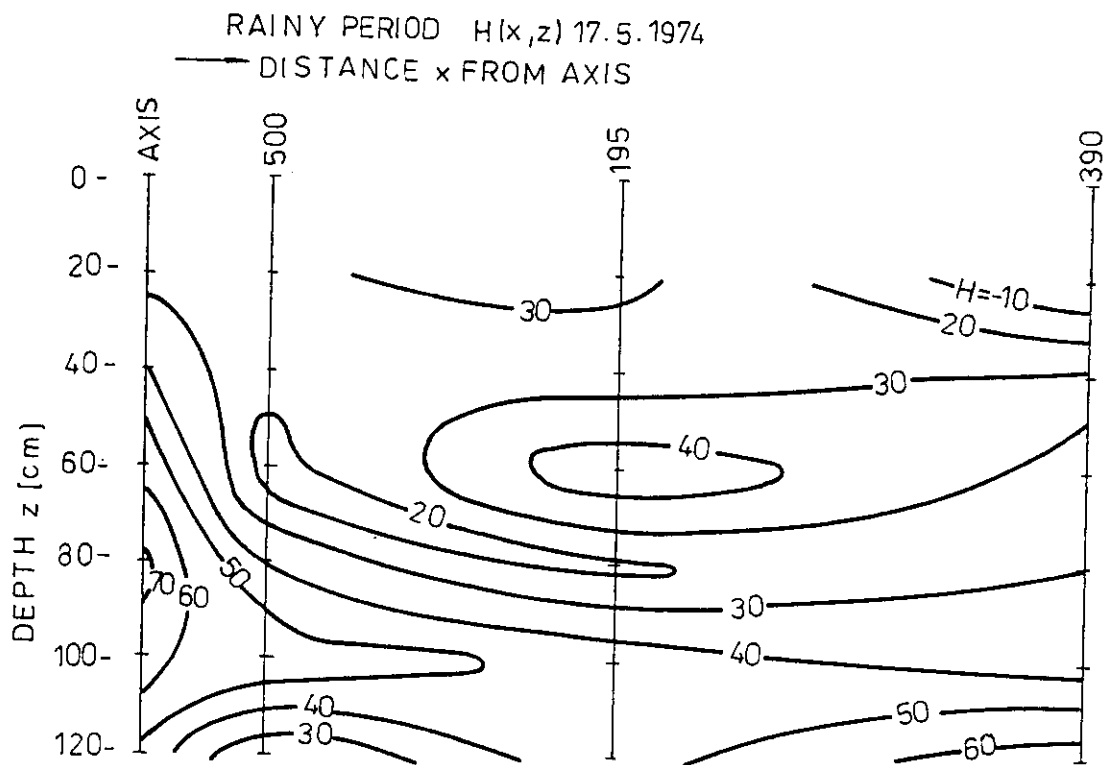
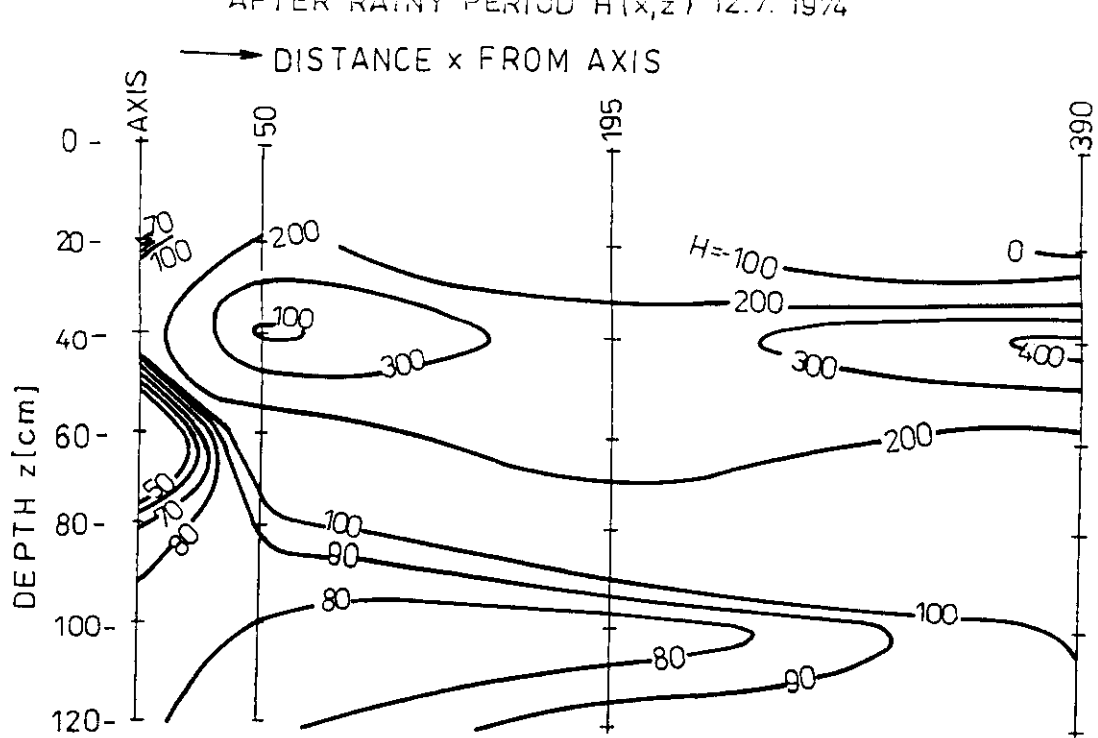


FIG. 3.4.b)

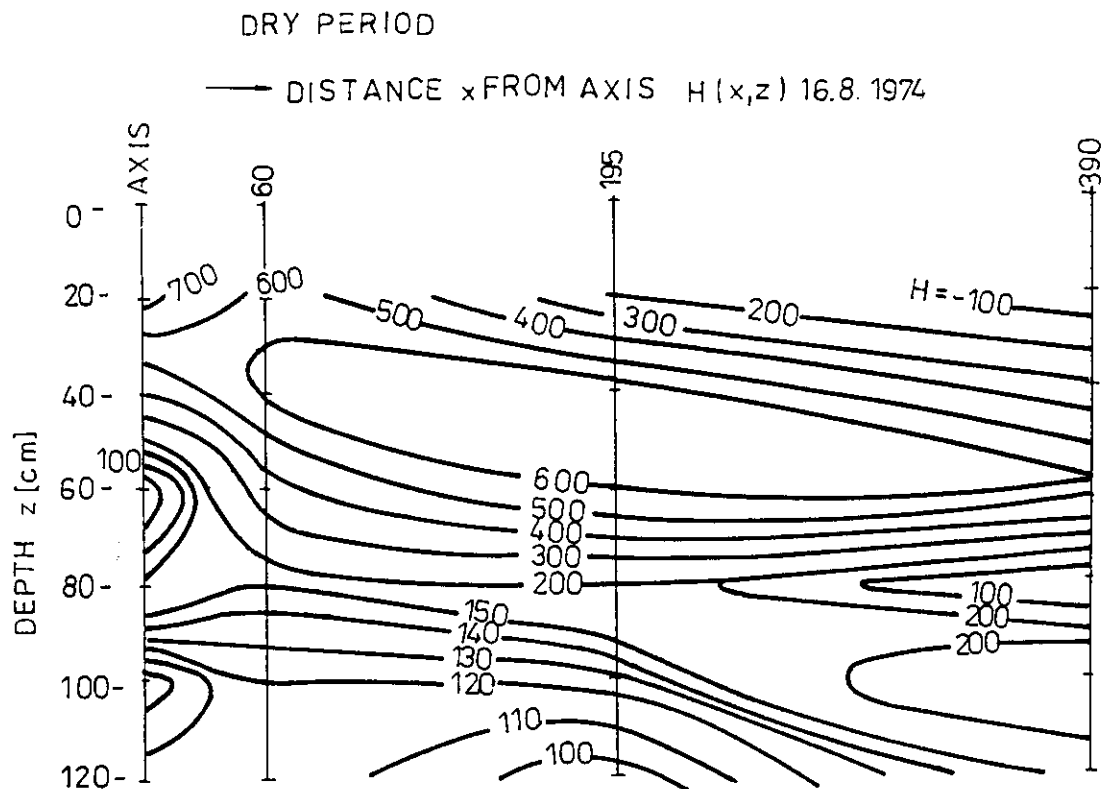
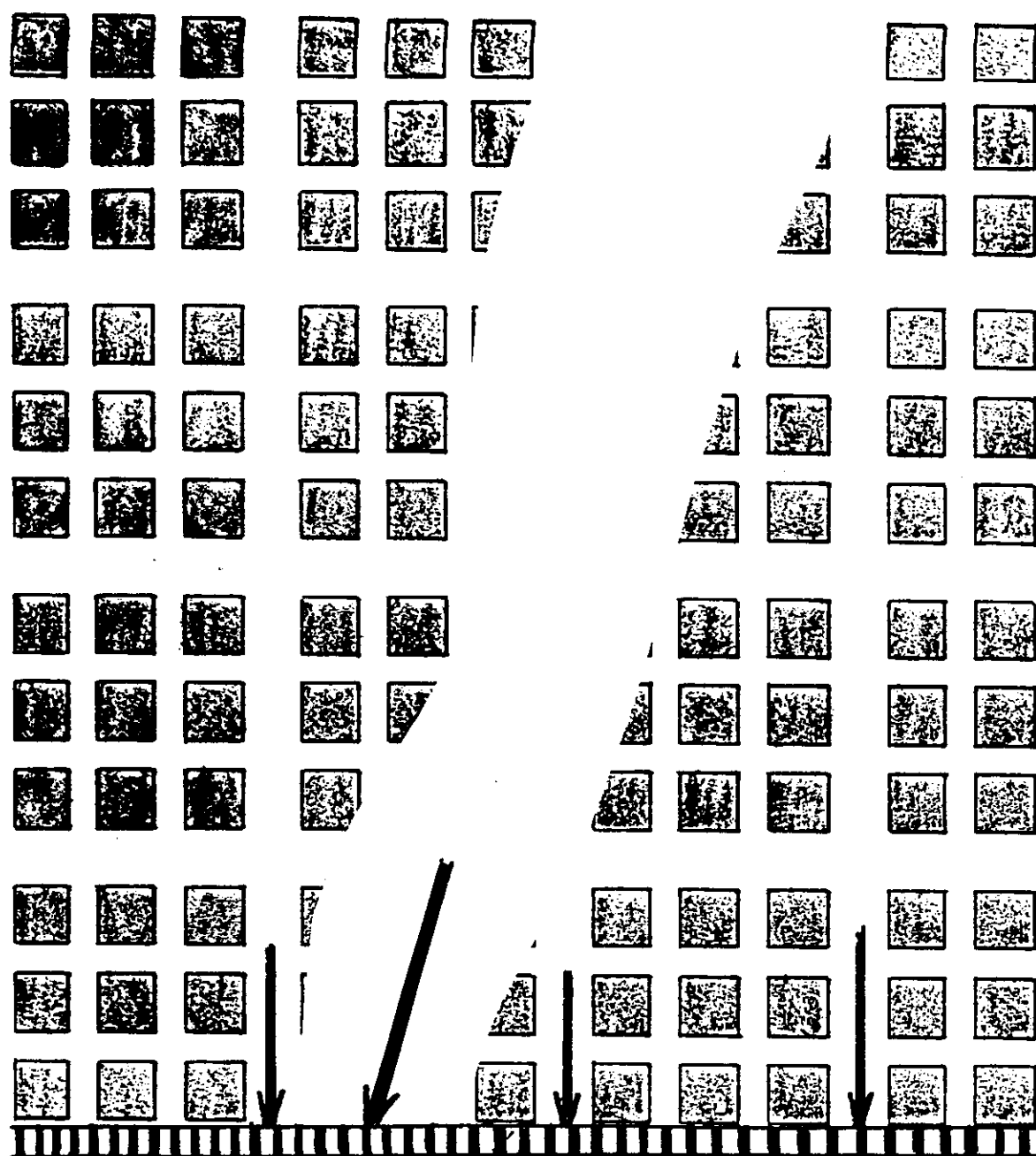


FIG. 3.4.c)



POROUS PLATE

SUCTION LYSIMETER

FIG. 3.5.

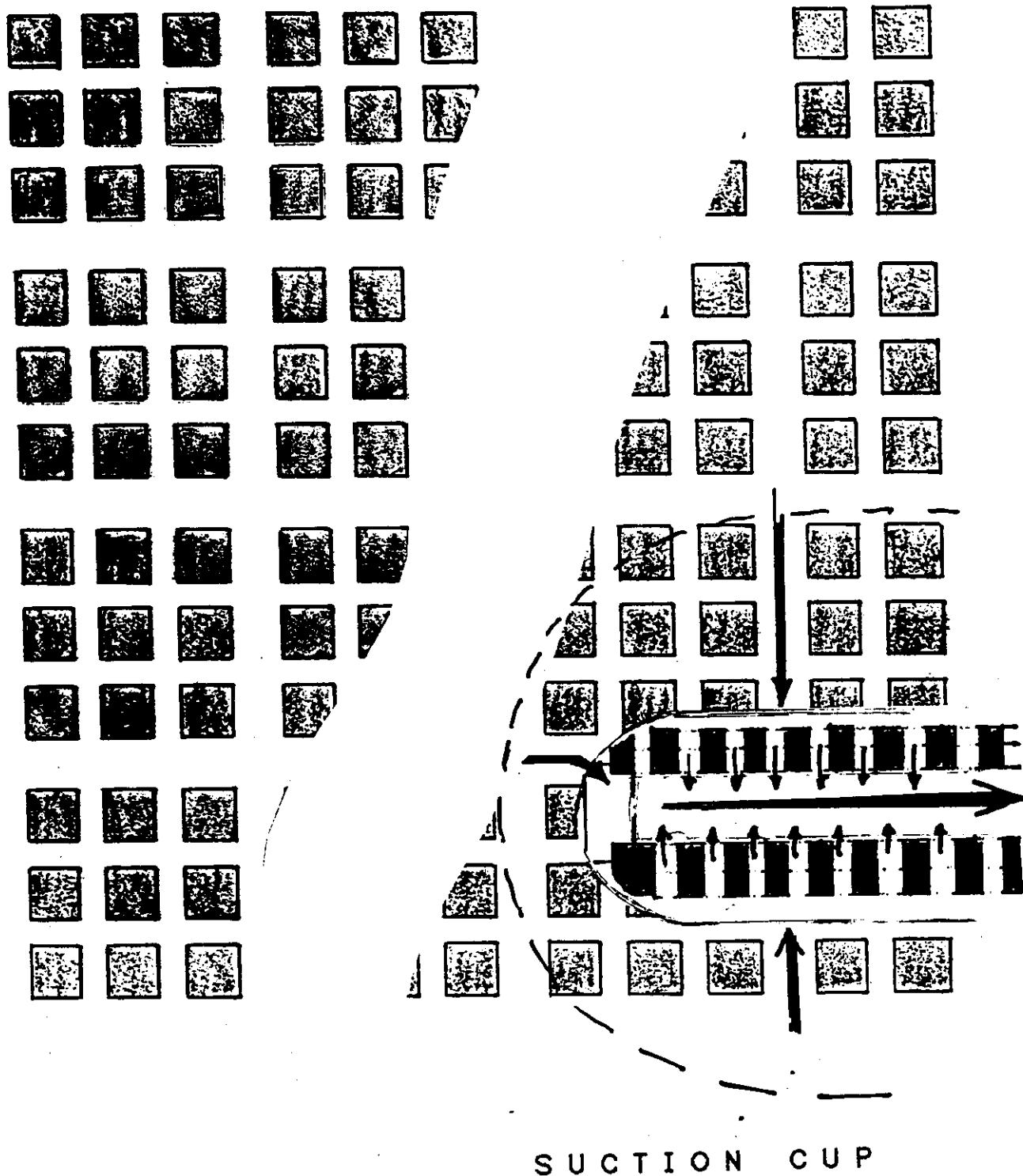
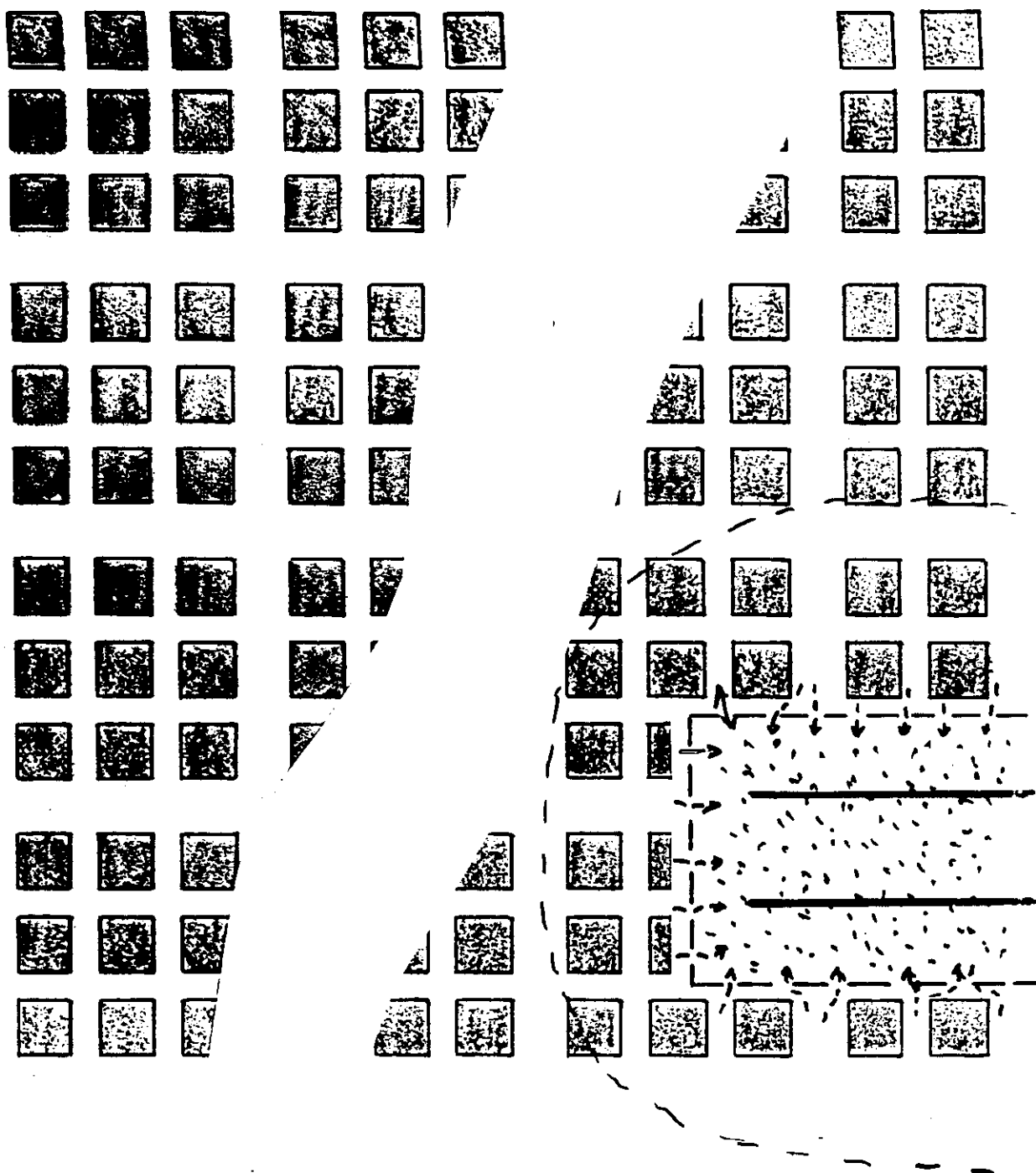


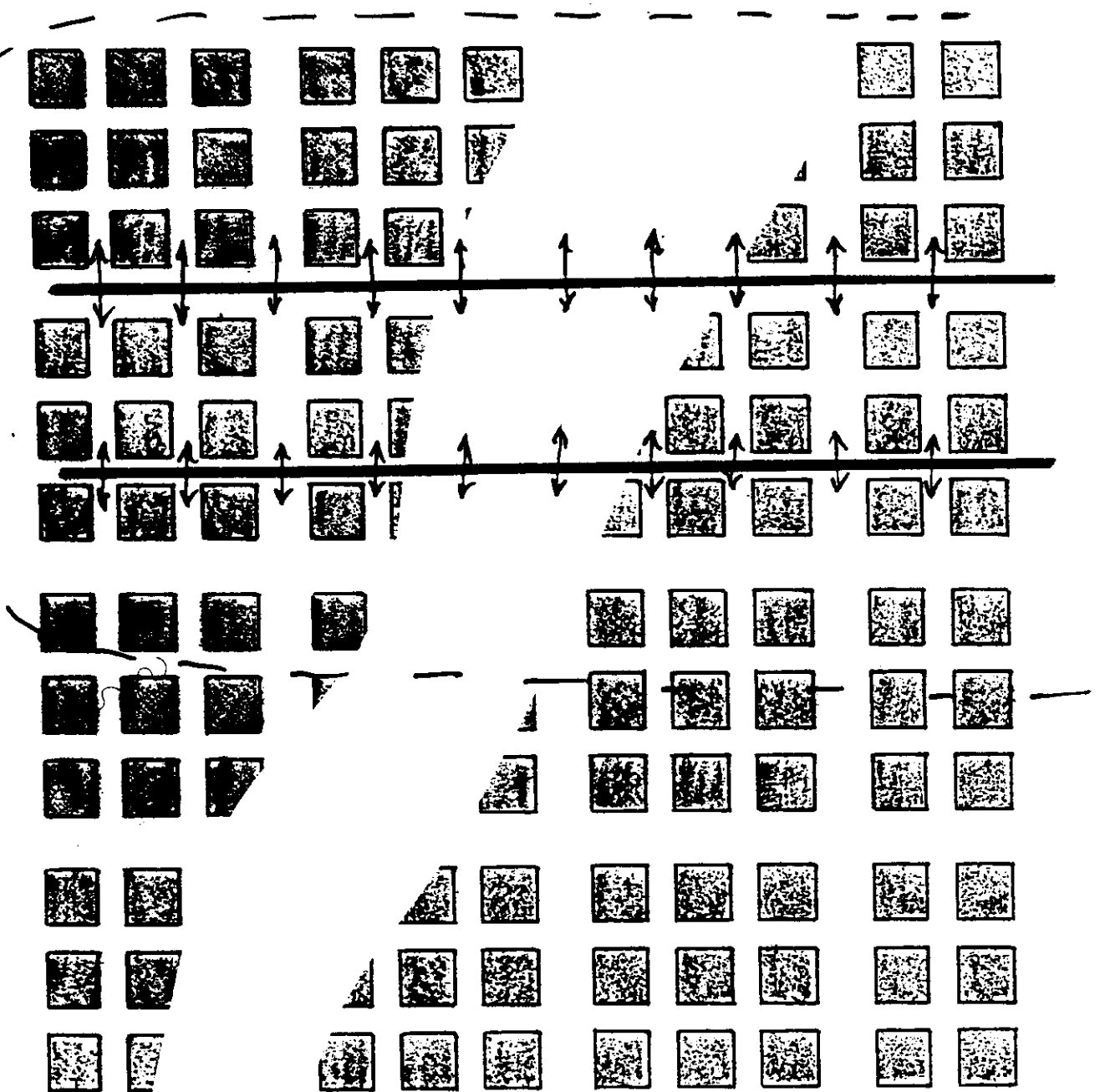
FIG. 3.6.





RESISTANCE BLOCK

FIG. 3.7.



T D R

FIG. 3.8.

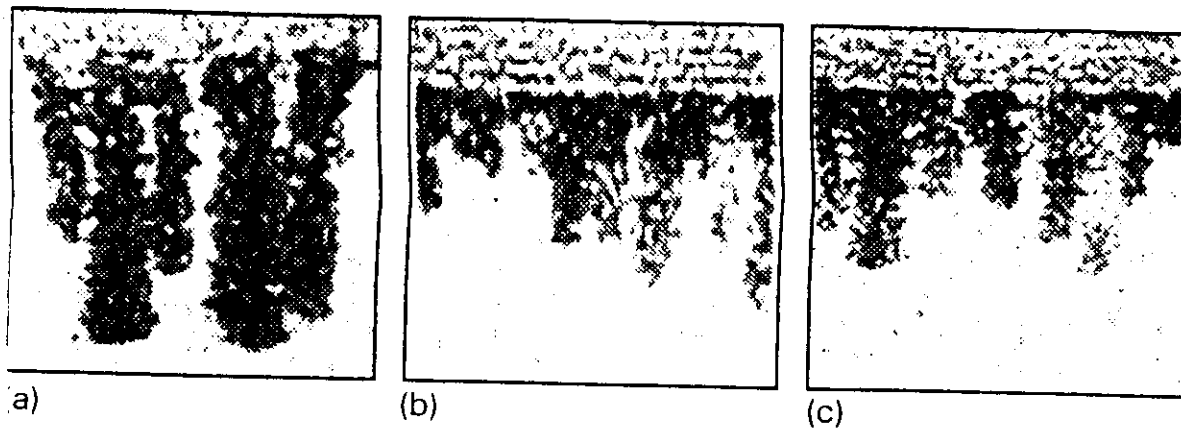


Fig. 2. Images obtained with the MRI system, showing three transverse sections of the fingering phenomenon in steady-state conditions. Each section represents a slice, 2.0 cm thick, 15.0 cm wide and 14.5 cm high, of the cubic soil column,  $15 \times 15 \times 15 \text{ cm}^3$ . We can clearly notice the spatial variability of the phenomenon in these three images. In (a) the fingers are close to the bottom of the box. In (b) and (c) they are close to the central part of the cubic column; still halfway to the bottom (Posadas, 1994).

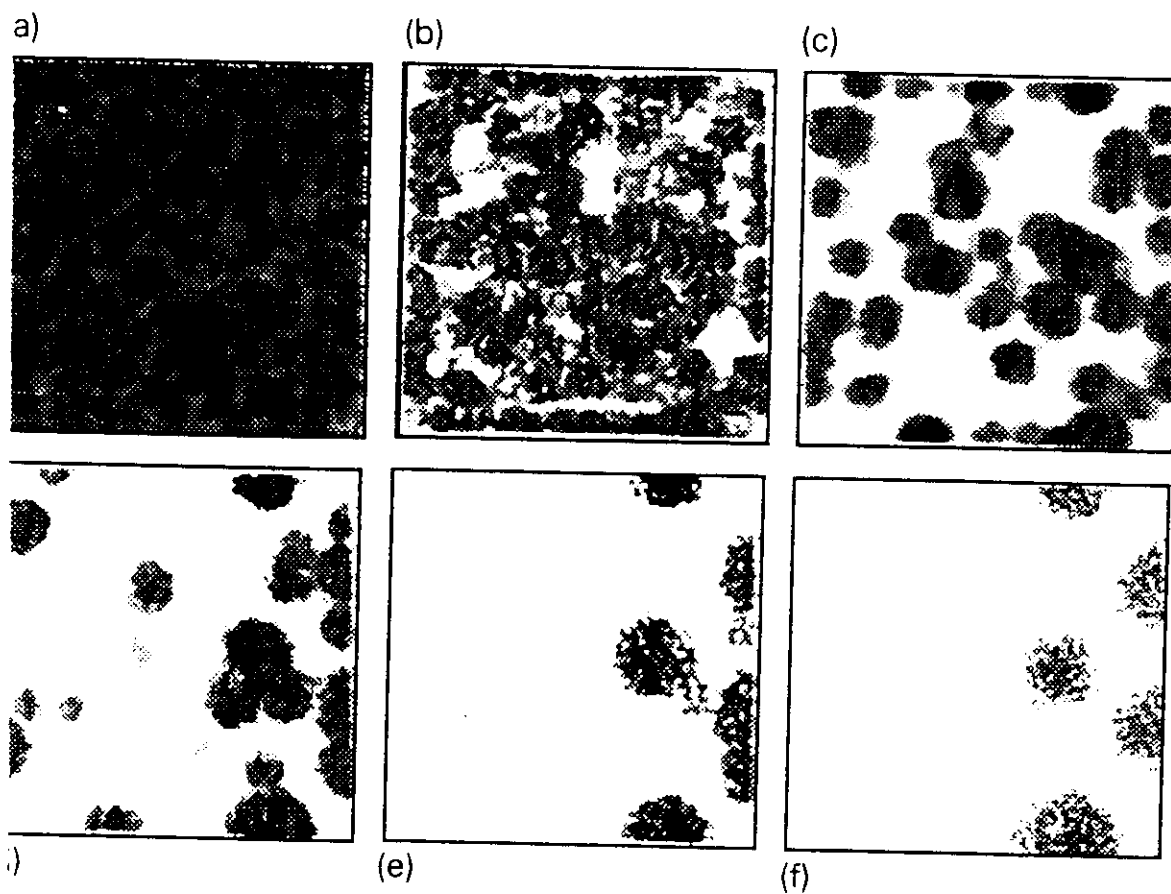
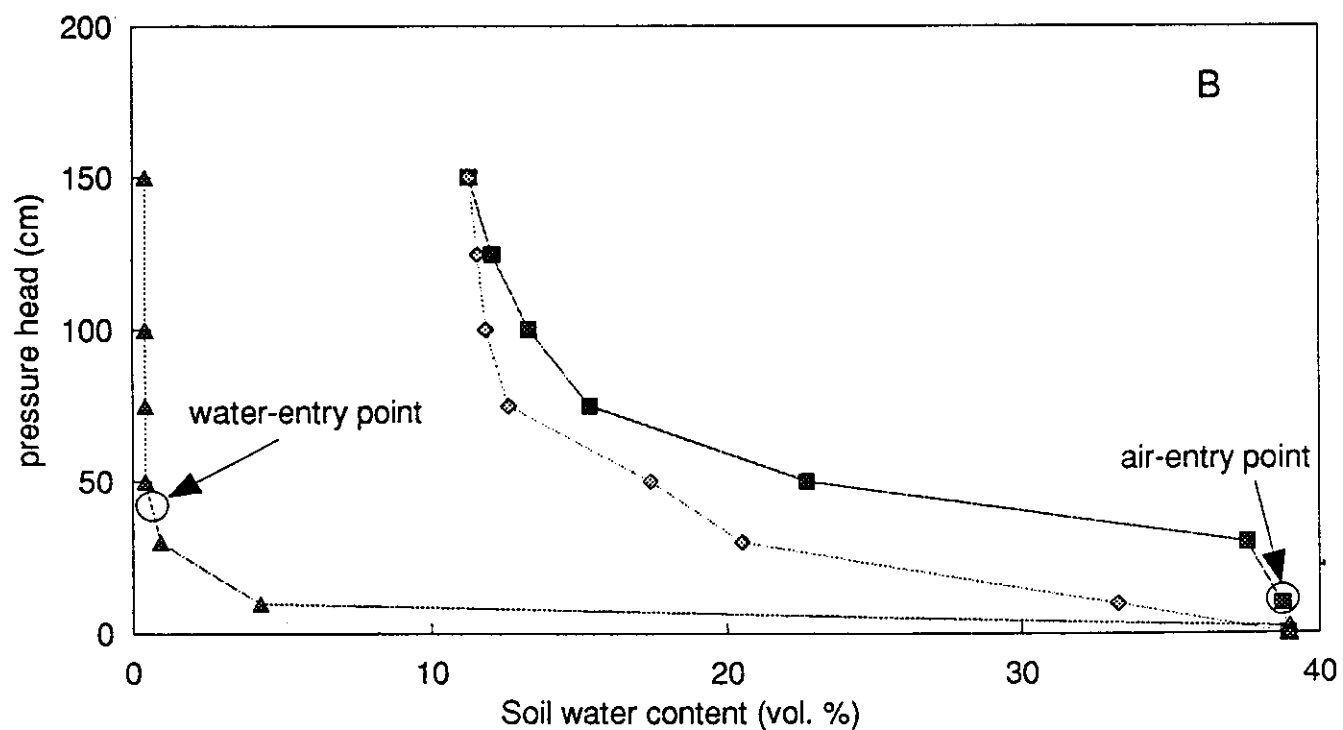
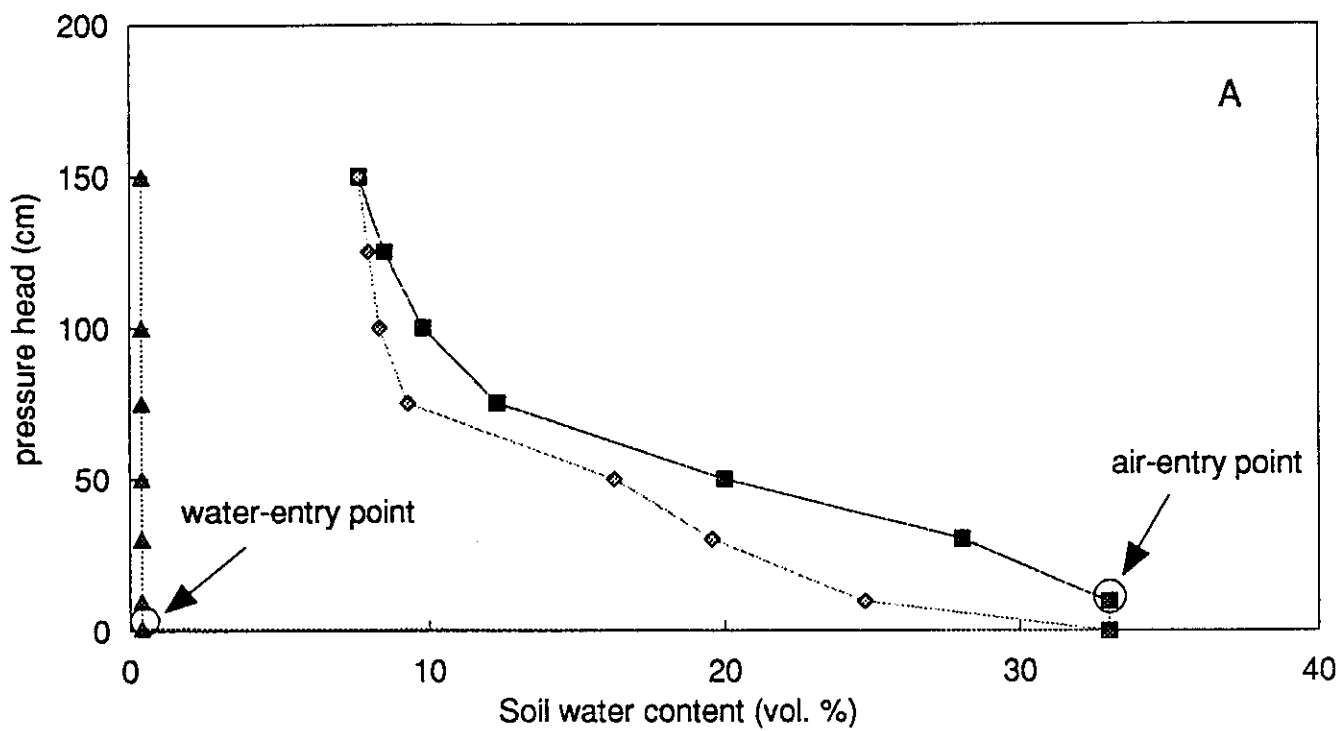


FIG. 3.9

Fig 3.10




Hysteretic water retention curves of the water repellent topsoil (A) and the wettable subsoil (B) at Vredepeel.

FIG. 3.10

## 4. ELEMENTARY SOIL HYDROLOGIC PROCESSES

---

**SH**  M. Kutilek & D.R. Nielsen: SOIL HYDROLOGY, Catena, 1994

---

### 1. INFILTRATION

Definition: **SH**, p. 133-134

- 1.1. Unsteady infiltration with Dirichlet's Boundary Condition (DBC), general information, **SH** p. 140-144.
  - 1.1.1. Analytical and semi-analytical solutions, **SH**, p. 144-150.
  - 1.1.2. Approximate solutions, **SH**, 153-158.
  - 1.1.3. Empirical equations, **SH**, 158-159.
- 1.2. Unsteady infiltration with Neuman's Boundary Condition (NBC), **SH**, 159-164.

### 2. REDISTRIBUTION

- 2.1. Soil water redistribution after infiltration, **SH**, p. 176-179.
- 2.2. Drainage to ground water table, **SH**, p. 181-182.
- 2.3. Field capacity, **SH**, p. 179-180.

### 3. EVAPORATION FROM A BARE SOIL

Definition, **SH**, p. 182-183.

- 3.1. Steady evaporation from a homogeneous soil profile, **SH**, p. 183-184.
- 3.2. Steady evaporation from a layered profile, **SH**, p. 185-187.
- 3.3. Unsteady evaporation, **SH**, p. 187-193.

## 5. SOIL SEALING AND CRUSTING

---

**SH**  M. Kutílek & D.R. Nielsen: SOIL HYDROLOGY, Catena, 1994

---

- 1.1. Description of the process, **SH**, p. 166-168.
- 1.2. Steady infiltration into crust-topped soil, **SH**, p. 136-139.
- 1.3. Unsteady infiltration into crust- and seal-topped soils, **SH**, p. 168-171.
- 1.4. Linked effects of infiltration into crust-topped soils:


Fingering.

Air exclusion at the crust-soil interface:

In some experiments on steady infiltration into crust-topped soil profile, an additional resistance has been observed in the vicinity of the interface between the crust and subsoil. This hydraulic resistance increases with time of infiltration. There is a hypothesis on release of air originally dissolved in water. Due to steep drop in water pressure across the crust, the dissolved air is released in microbubbles which are blocking some pores. Consequently, hydraulic resistance increases, the value of the increased resistance is in some instances 3 to 4 times higher than was the initial resistance of the crust.

## 6. SOIL HYDROSTATICS: FROM PARALLEL TUBE MODELS TO FRACTAL FRAGMENTATION AND PERCOLATION MODELS

---

**SH**  M. Kutilek & D.R. Nielsen: SOIL HYDROLOGY, Catena, 1994

---

### Models of soil water retention curves (SWRC):

1. SWRC is linked to summation curve of particle size (diameter) distribution (SPDD):
  - 1.1. Either formally on geometric similarity of SWRC to SPDD.
  - 1.2. Or, models consist of spherical particles. Between them hypothetical pores exist. For both instances we have to determine empirically fitting parameters in order to obtain good agreement between measured and modeled SWRC. The transition from hydrostatics (i.e. from SWRC) to hydrodynamics (i.e.  $K_S$  and  $K(\theta)$ ) is just empirical and theoretical solution is not feasible. All fitting parameters are valid for the certain pedotop, for which they were derived.
2. SWRC models based directly on soil porous systems, **SH** p. 79-85.:
  - 2.1. Bundle of parallel tubes with distinct pore size classes (Childs and Collis-George, 1950), **SH** Fig. 4.19, p. 79, or in later development the modelers worked with continuous pore size distribution (PSD), see Mualem (1976), **SH** p. 106-108, with eventual interconnection of tubes.
  - 2.2. Percolation in disordered networks, **SH**, p. 80-81. Simple examples of percolation, Fig. 6.1. to 6.3, hierarchical arrangement, Fig. 6.4, 6.5. Main disadvantage: If we want to use a network model of a real soil and on a real soil, we have to know PSD. However, PSD from image analysis is 2-dimensional and not fully reliable for 3-dimensional models. PSD from mercury porosimetry is derived from bundle of parallel tubes. The same is for SWRC.
  - 2.3. Fractal fragmentation: From soil structure construction by fractal fragmentation (virtual soil samples) to porous system (Perrier et al., 1995, 1996). Fragmentation starts with a set of initial points in a square  $P_0$ , Fig. 6.6 (a). Then a space partition is made in order to split  $P_0$  into polygonal zones  $P(M)$ , each associated with point  $M$  (Voronoi tessellation, or Thiessen polygon in hydrology), Fig. 6.6 (b). Then a porous structure is created with  $P(G, k)$ .  $G$  is the center of gravity,  $k$  is chosen to generate the given porosity. If  $k$  is proportional to initial distribution of polygonal zones, then PSD is simply associated to SPDD, Fig. 6.6 (c). This process can be repeated on successive levels of fragmentation. What were earlier solid elements  $P(M)$  are now aggregates that may be divided into smaller microaggregates or particles, Fig. 6.6 (d). The final fractal structure is defined by fractal dimension  $D$ .  $N$  polygons in 2-dimensions correspond to  $n = N^{3/2}$  in 3-dimensions,  $r = k N^{1/2}$  in isotropic material and the fractal dimension is then  $D = -\log n / \log r$ . SWRC equation of Rieu and Sposito (1991), quotation in **SH** is

$$\theta(h) = (h h_s)^{D-3} + \theta_s - 1$$

The modeled data fit very well to this eq. Earlier expressions based on Brooks and Corey eq.

$$\theta(h)/\theta_s = (h/h_s)^{D-3}$$

look as less appropriate, especially when we consider the empirical value of the exponent in Brooks and Corey eq., which is usually in ranges -2 to -5. If percolation theory is applied for the description of the invading fluid into multi-level fragmented model, n-modal SWRC is obtained, including the hysteretic loop, see Fig. 6.8.

### Additional references

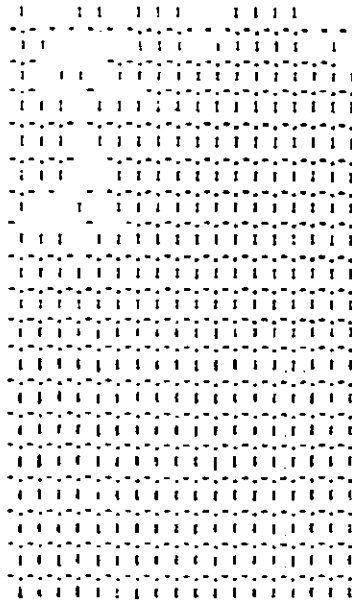
- Perfect, E., B. D. Kay and V. Rasiyah, 1993. Multifractal model for soil aggregate fragmentation. *Soil Sci. Soc. Am. J.*, 57:896-900.
- Perrier, E., C. Mullon, M. Rieu and G. de Marsily, 1995. Computer construction of fractal soil structures: Simulation of their hydraulic and shrinking properties. *Water Resour. Res.* 31:2927-2943.
- Perrier, E., M. Rieu, G. Sposito and G. de Marsily, 1996. Models of the water retention curve for soils with a fractal pore size distribution. *Water Resour. Res.* 32:3025-3031.
- Yanuka, M. 1992 Percolation theory approach to transport phenomena in porous media. *Transport in Porous Media* 7:265-282.



# INCREASING EQUILIBRIUM PRESSURE

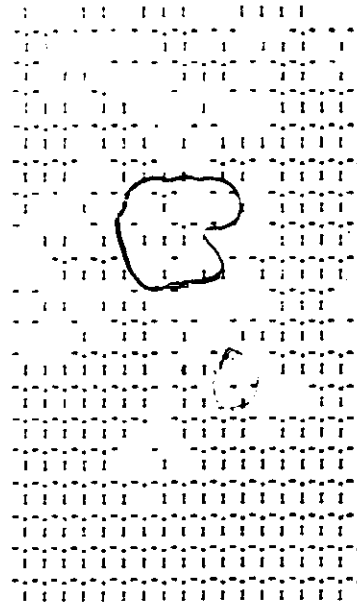
$$p_1 < p_2 < p_3 < p_4$$

$p_1$



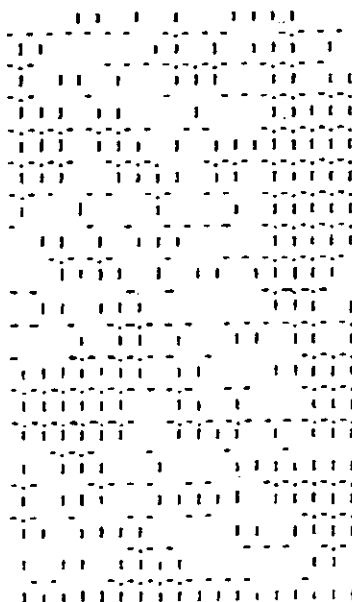
**a**

$p_2$



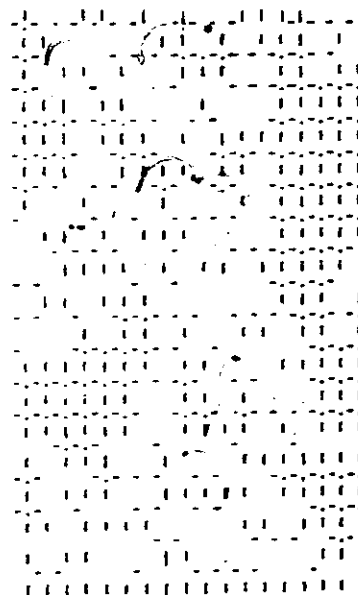
CLUSTERS  
OF **b**  
ISOLATED WATER

$p_3$



**c**

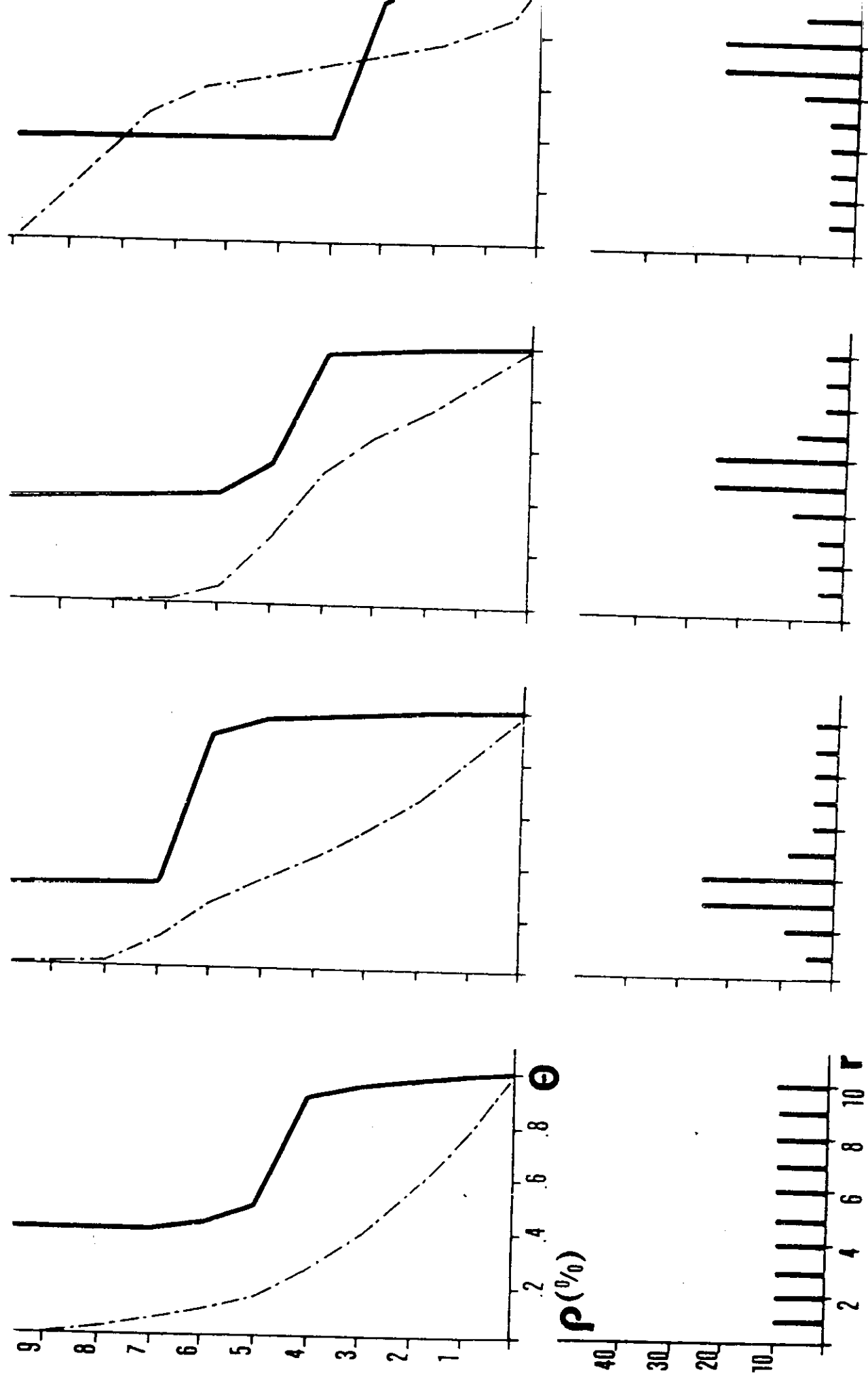
$p_4$



**d**

FIG. 6.1

FIG. 6.2



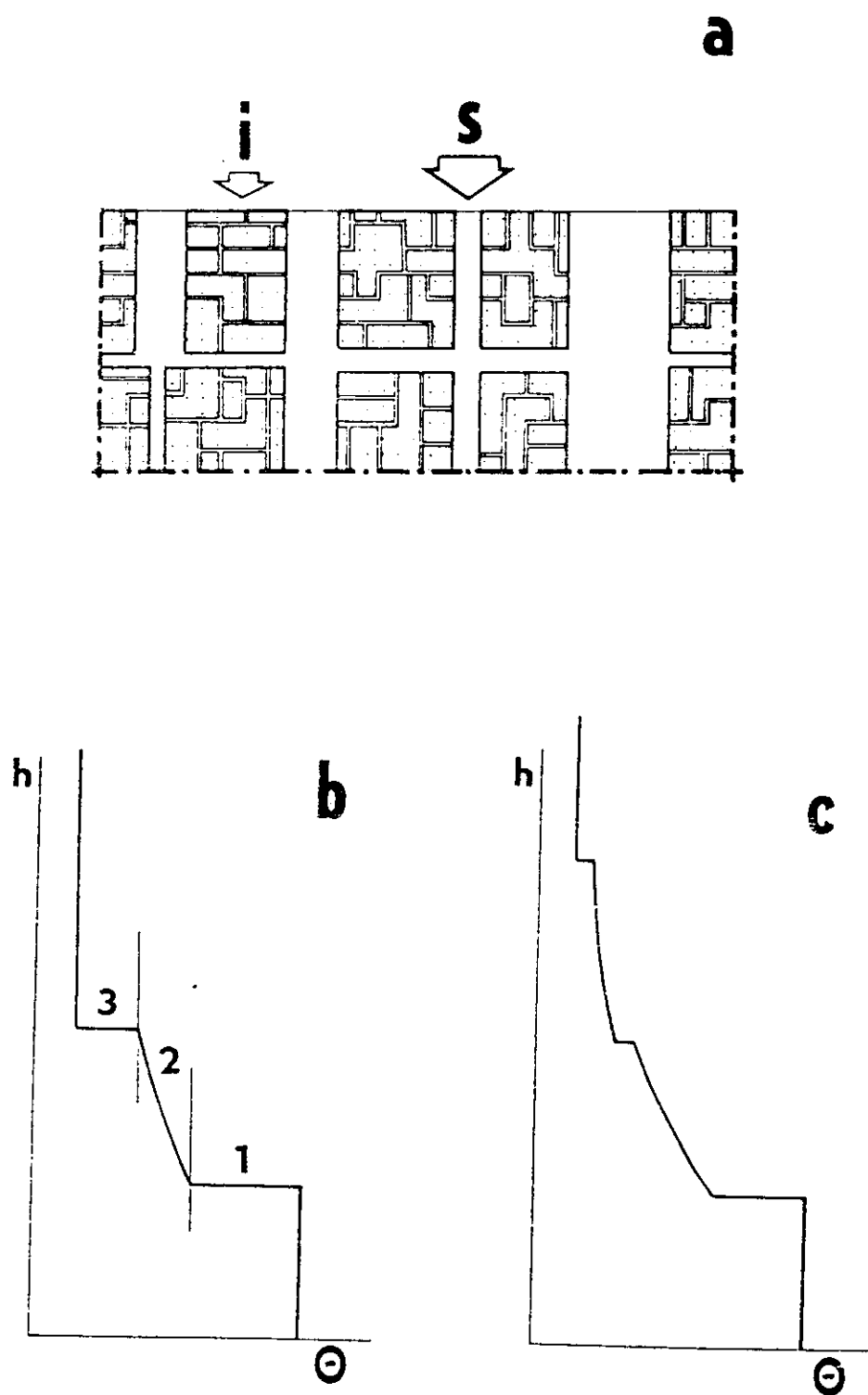


FIG. 6.3.

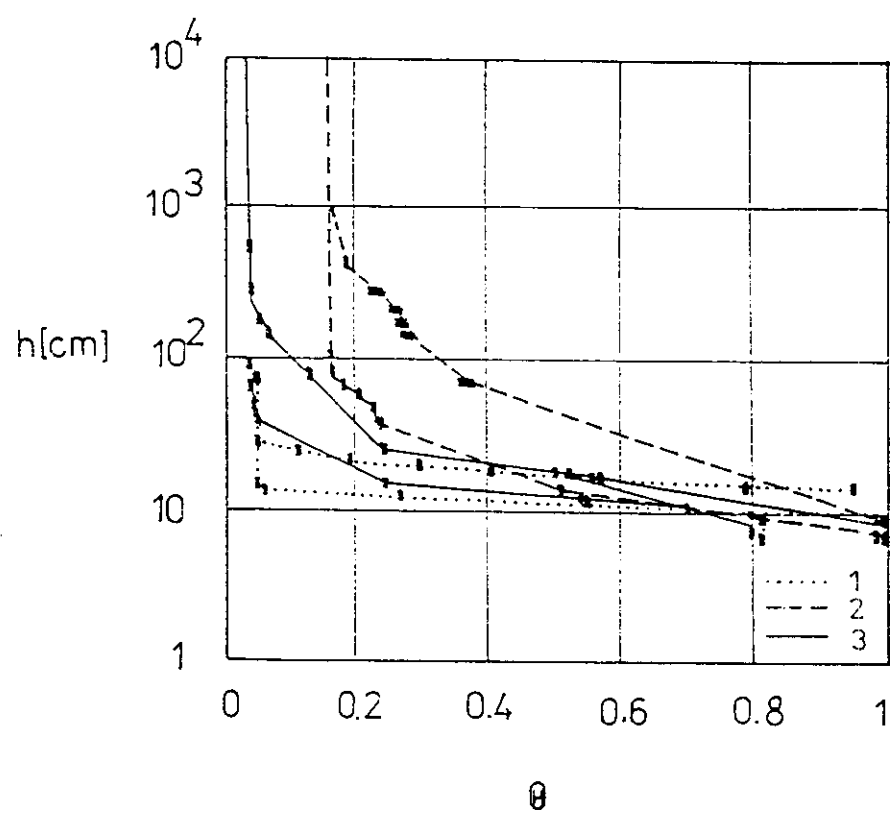


FIG. 6.4.

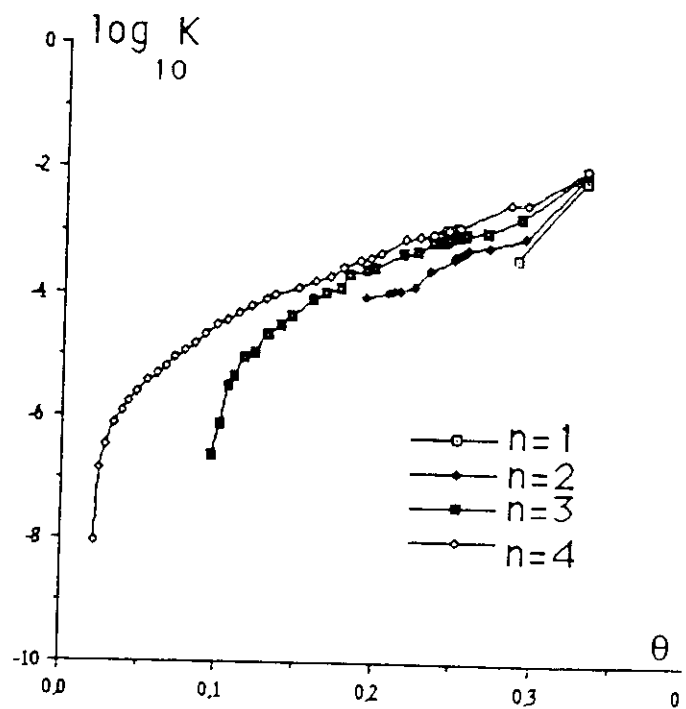
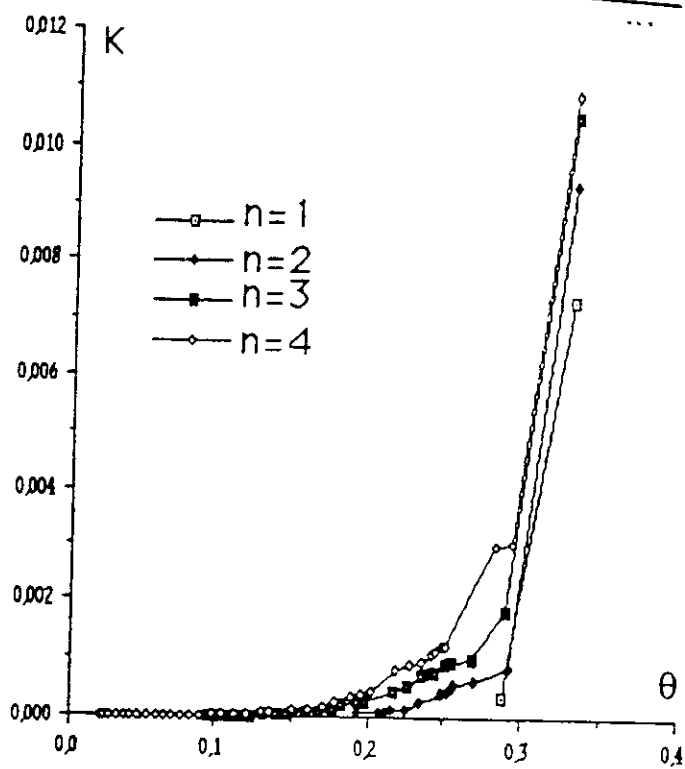
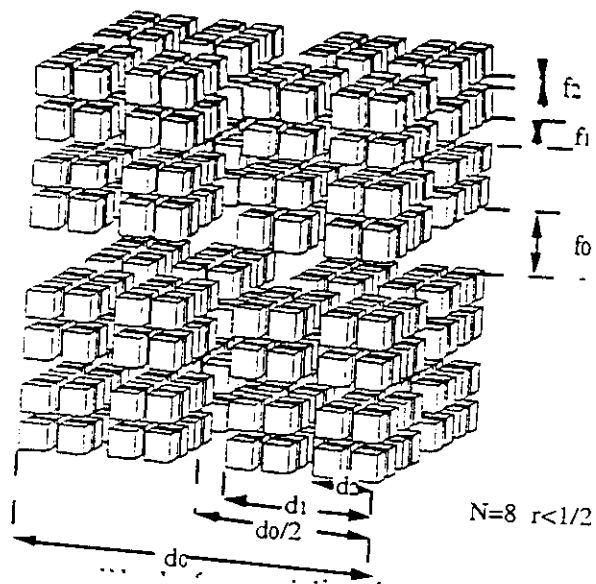


FIG. 6.5.a)

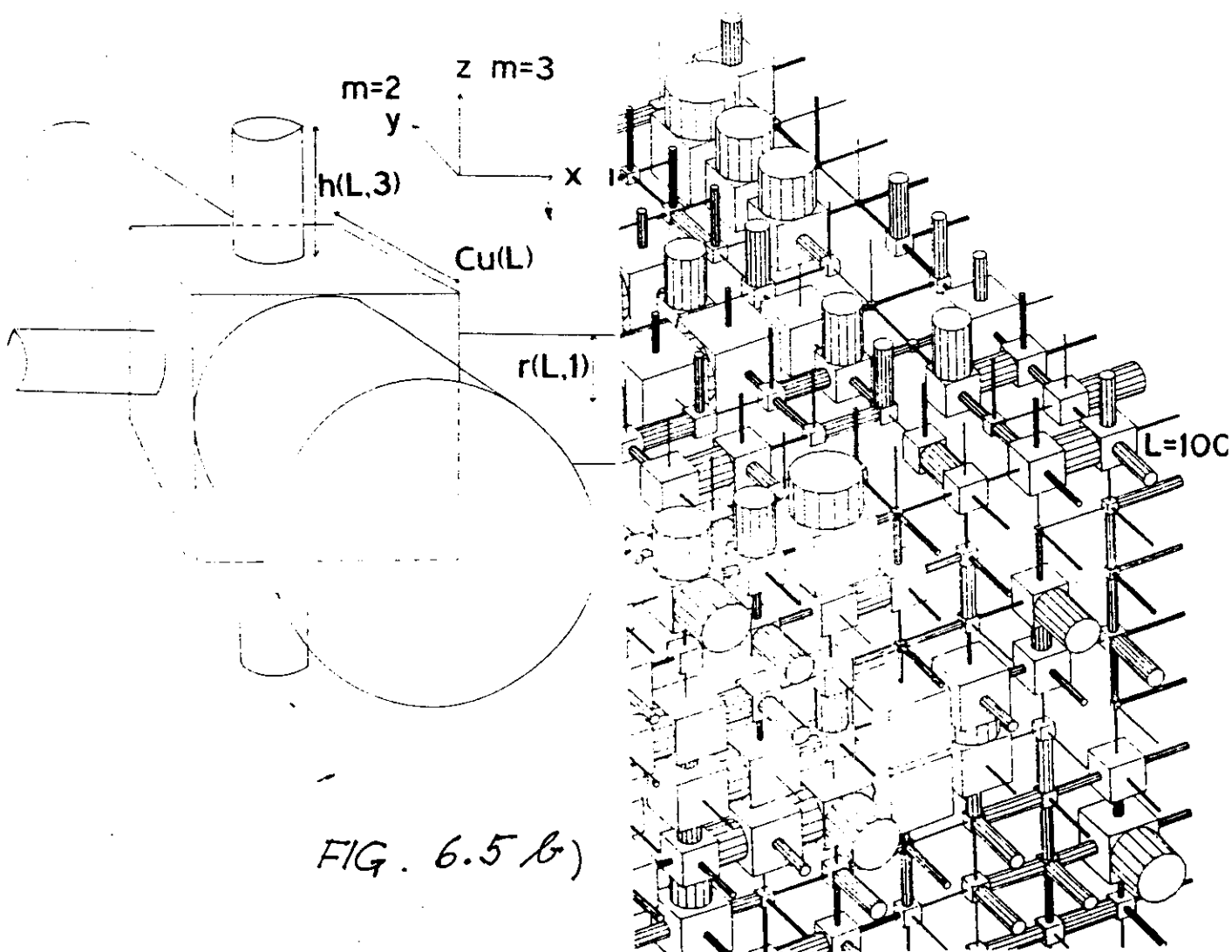
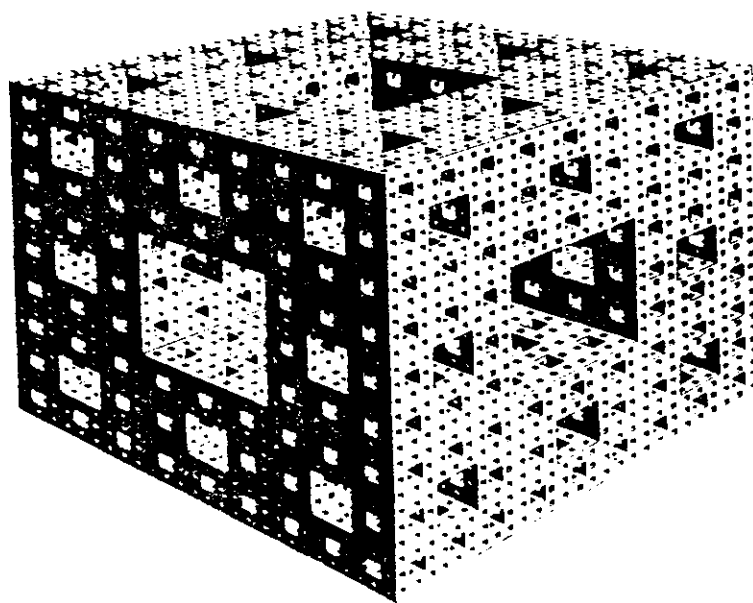
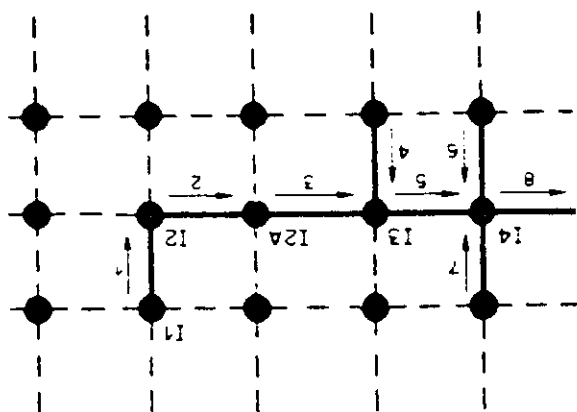
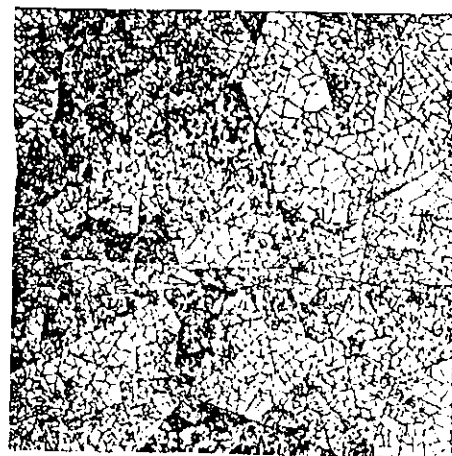
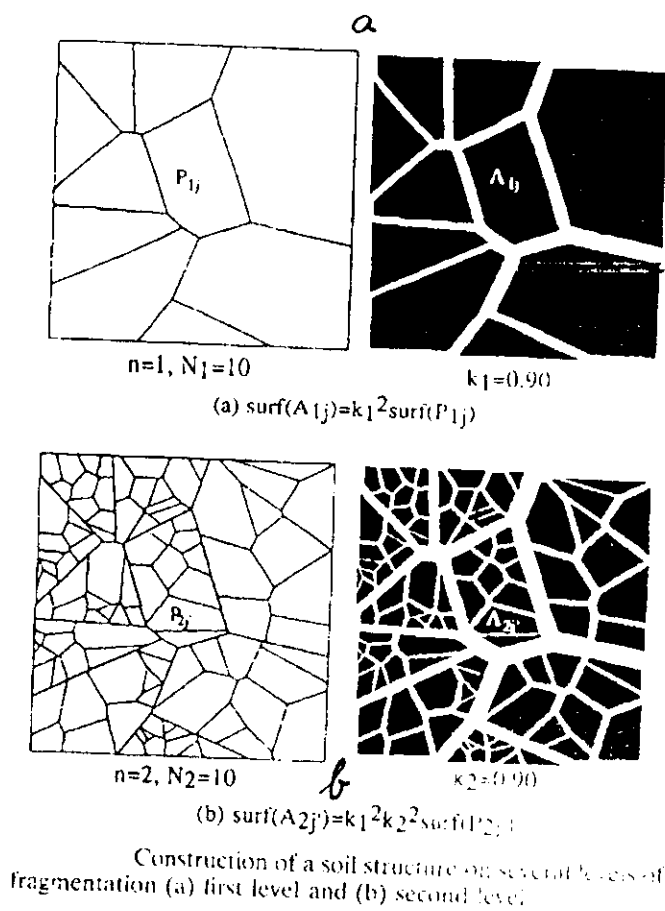
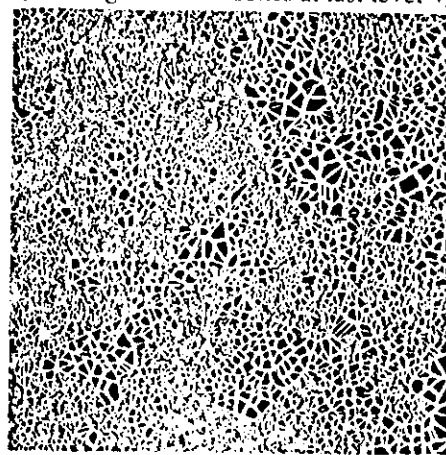


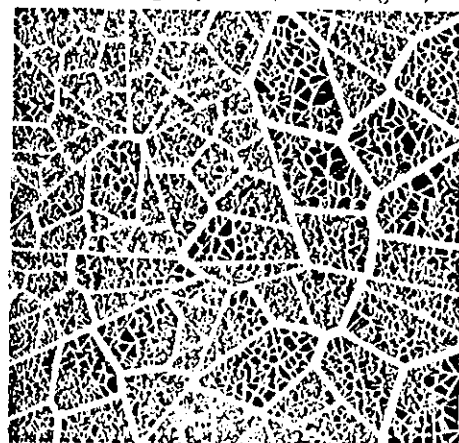
FIG. 6.5 b)



(a)  $n=4, N_1=N_2=N_3=N_4=10$   
( $10^4$  fragmentation zones at last level 4)



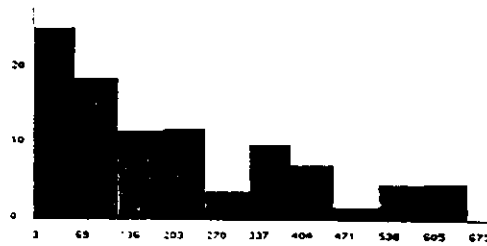
(b)  $k_1=k_2=k_3=1, k_4=0.85$  ( $k_0=1$ )



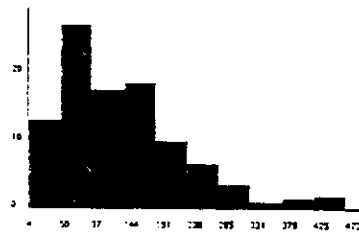
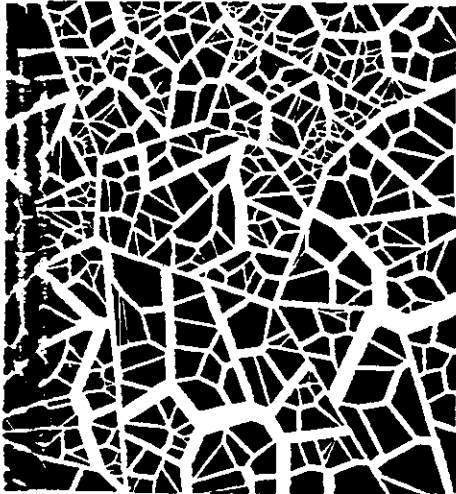
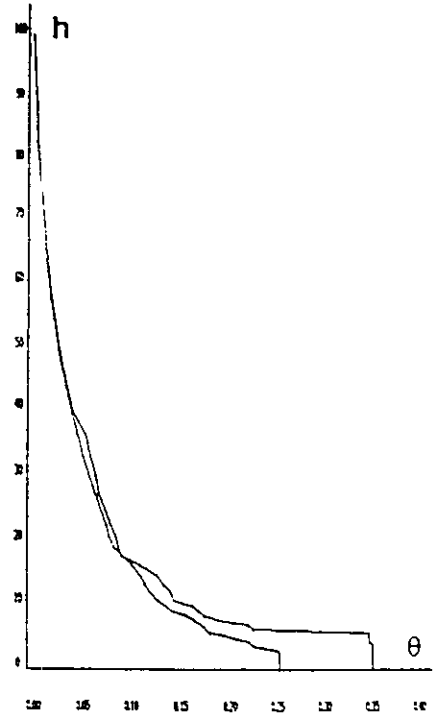
(c)  $k_1=1, k_2=0.92, k_3=1, k_4=0.92$  ( $k_0=1$ )

Different soil structures associated with the same particle size distribution (PSD), same total porosity and different pore size distribution (psd). (a) structure skeleton, (b) first example of associated structure with no visible aggregates, and (c) second example of structure with a homometric ratio  $k_2 \neq 1$  defining aggregates of particles at level 2.

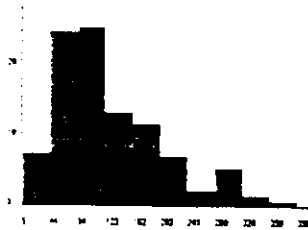
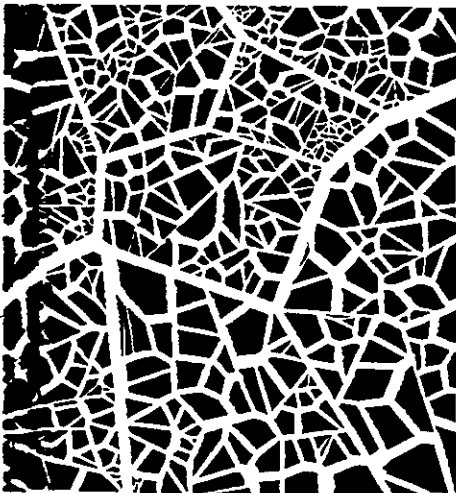
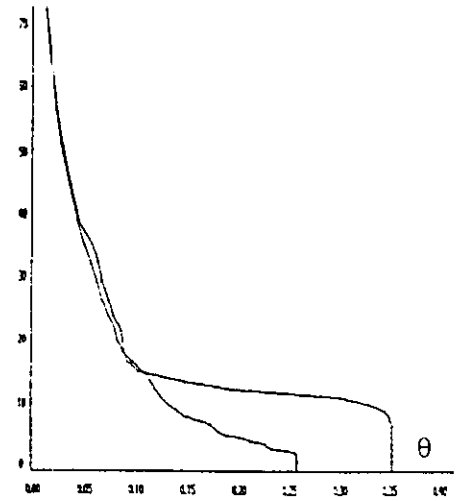
FIG. 6.6



(a) Etat saturé scénario 1



b) Etat saturé scénario 2'



c) Etat saturé scénario 2''

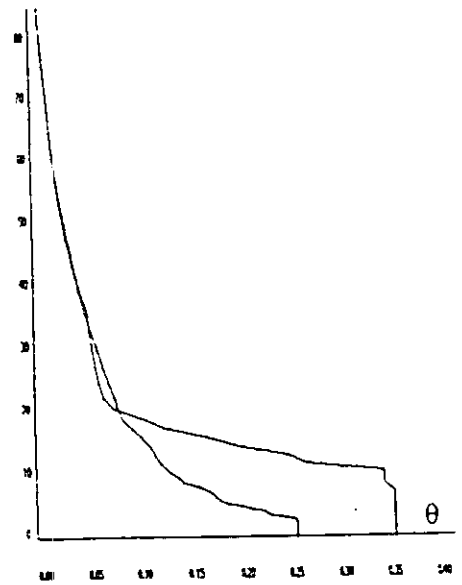
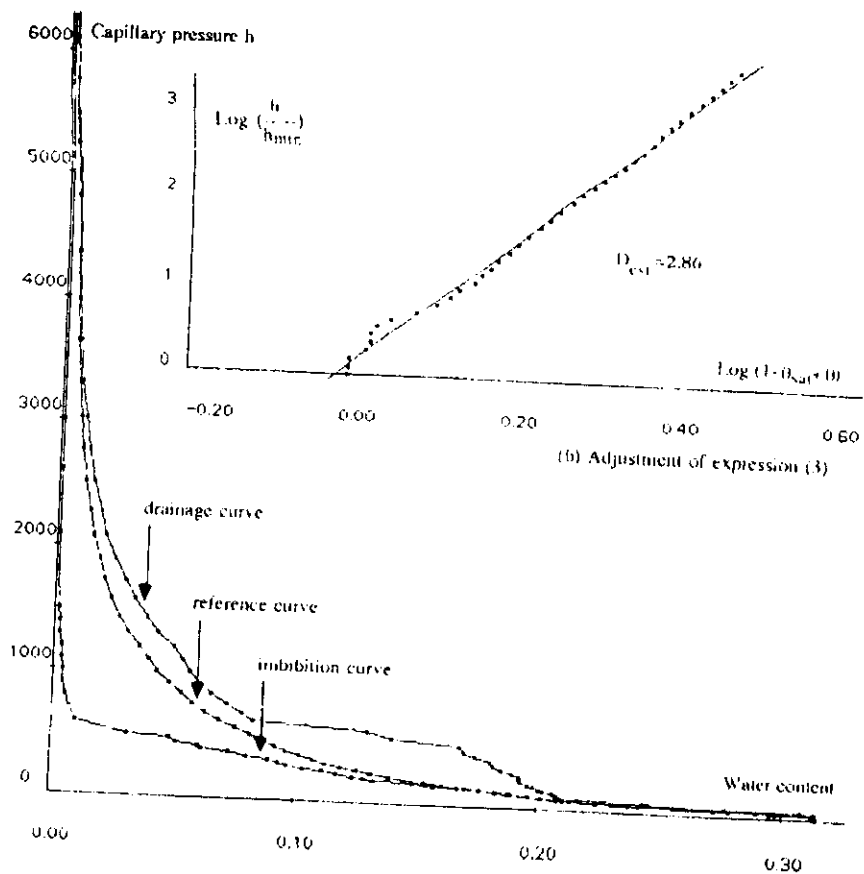


FIG. 6.7



PRESSURE HEAD  
 $h$  [cm]



$$K_r = \frac{K(\theta)}{K_s}$$

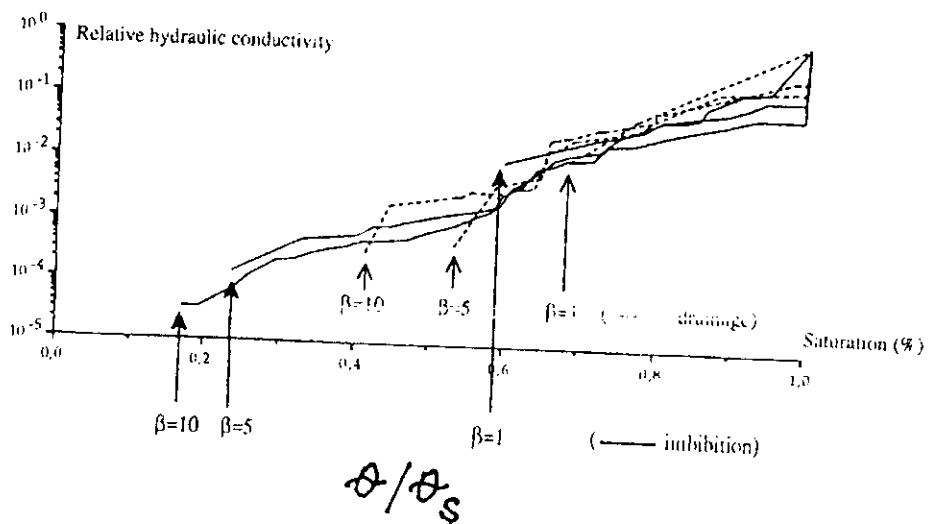


FIG. 6.8

## 7. THE SCALE OF OBSERVATION AND MODELING IN SOIL HYDROLOGY

---

**SH** M. Kutilek & D.R. Nielsen: SOIL HYDROLOGY, Catena, 1994

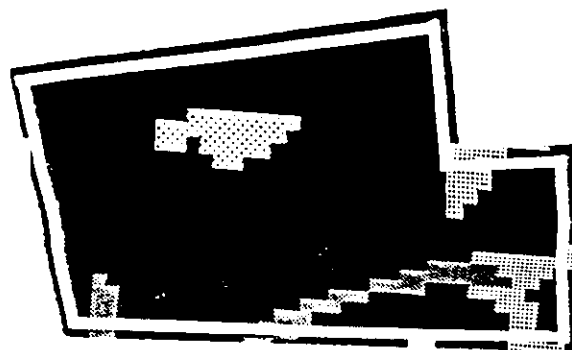
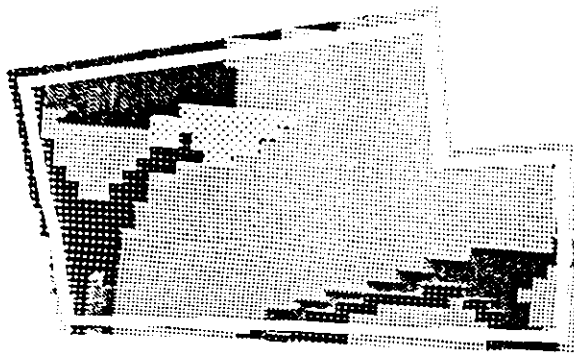
---

Definition of scale, **SH**, p. 13-15 and p. 251.

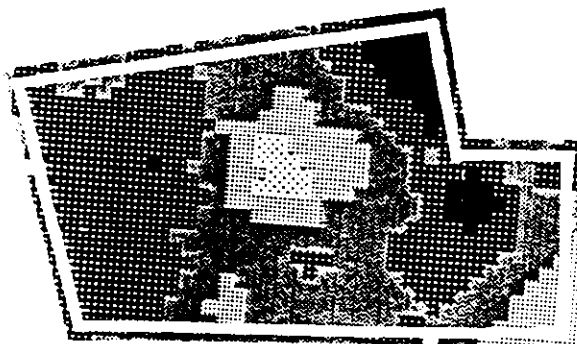
1. Pore scale, Navier-Stokes eq.
  2. Darcian scale
    - 2.1. Surrogate soil scale: Artificial porous materials, laboratory columns with repacked soil. Darcy-Buckingham eq., Richards eq.
    - 2.2. Pedon scale. Darcy-Buckingham eq., Richards eq.
  3. Pedotop scale: Geostatistics, **SH**, 252-262. Scaling applied to physical soil properties. Scaling applied to boundary conditions of elementary soil hydrologic processes, **SH**, 262-268. Probability density function (PDF) of estimates of soil hydraulic characteristics, see next table. Semivariance on „pedotop“ scale, Fig. 7.1. (Rogowski, Wolf, 1994)
  4. Mapping unit scale, **SH**, Fig 1.2. and 1.3., p. 14.
  5. Watershed scale.
  6. Regional scale.
- For scales > pedotop scale see ~~Fig. 7.2-7.4~~ <sup>7.1.</sup> (Rogowski, Wolf, 1994)

### Additional references

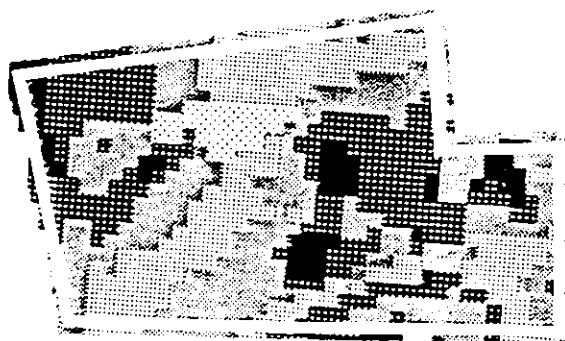
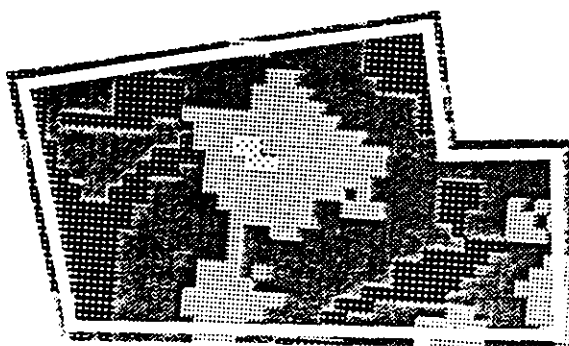
- Nielsen, D.R., M. Kutilek, and M.B. Parlange, 1996. Surface soil water content regimes: Opportunities in soil science. *J. Hydrol.* 184:35-55.
- Rogowski, A.J. and J.K. Wolf, 1994. Incorporating variability into soil map unit delineation. *Soil Sci. Soc. Am. J.* 58:163-174.



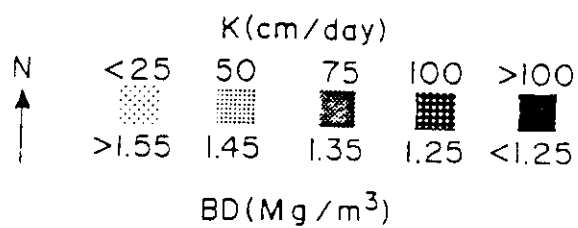
(a) SOIL SURVEY



(b) KRIGED



(c) COMBINED



ons of bulk density and hydraulic conductivity at a farm scale based on (a) the soil survey, (b) kriged  
lays of soil survey and kriged values.

FIG 7.1

TABLE 7.1.

## SCALE: ONE PEDOTOP

PDF of saturated hydraulic conductivity  $K_s$  [ $LT^{-1}$ ] and of sorptivity  $S$  [ $LT^{-1/2}$ ] estimated from ponded infiltration test by various infiltration equations

	arenic chernozem		ferralsol		
	short set	full set	A-B	C-D	full set
$K_s$					
Philip, 2-parameters	LG	-	LG	E	LG
3-parameters	W	B	LG	E	LG
Swartzendruber	B	W	LG	E	LG
Green-Ampt	-	-	LG	G	E
Brutsaert	W	-	LG	LG	LG
$S$					
Philip, 2-parameters	LG	W	G	N	N
3-parameters	LG	E	G	N	E
Swartzendruber	LG	E	G	N	E
Brutsaert	LG	-	LG	G	E

Types of PDF: N - normal

LG - log-normal

W - Weibull

G - gamma

B - beta


E - Erlang

PDF (A)  $\neq$  PDF (A +  $e_i$ )

(A +  $e_i$ ) is our estimate

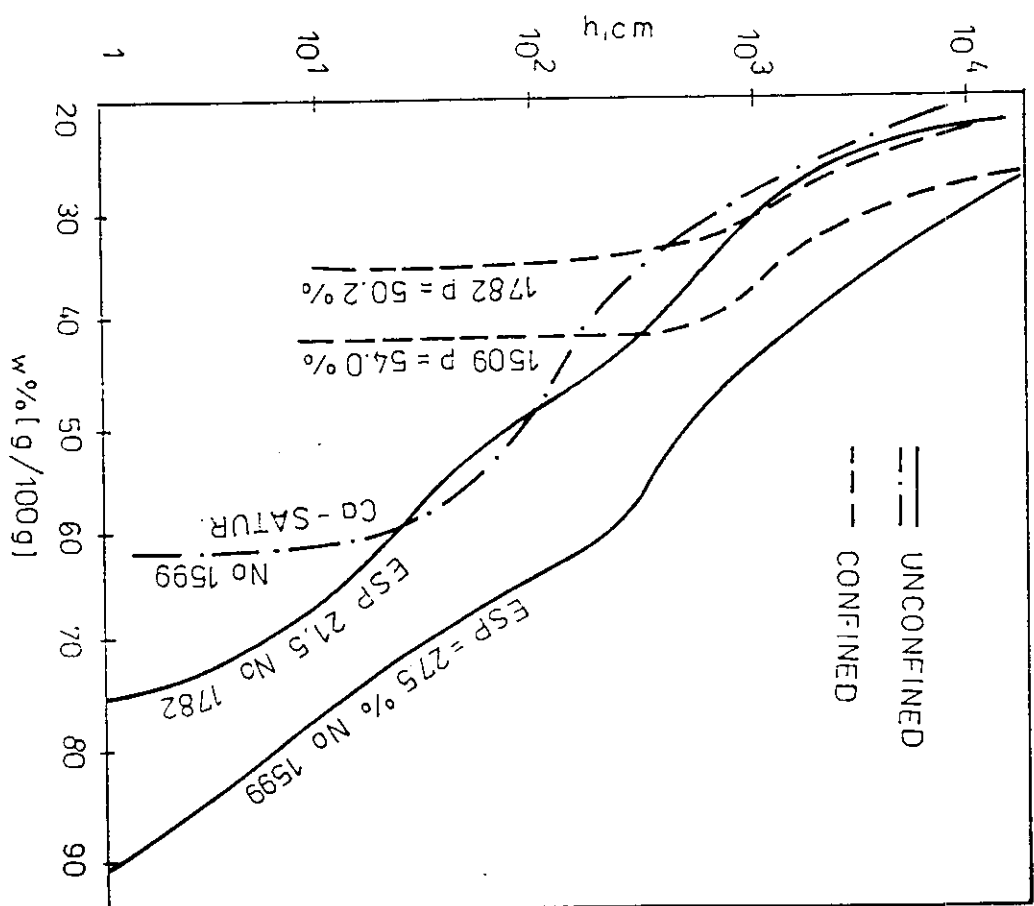
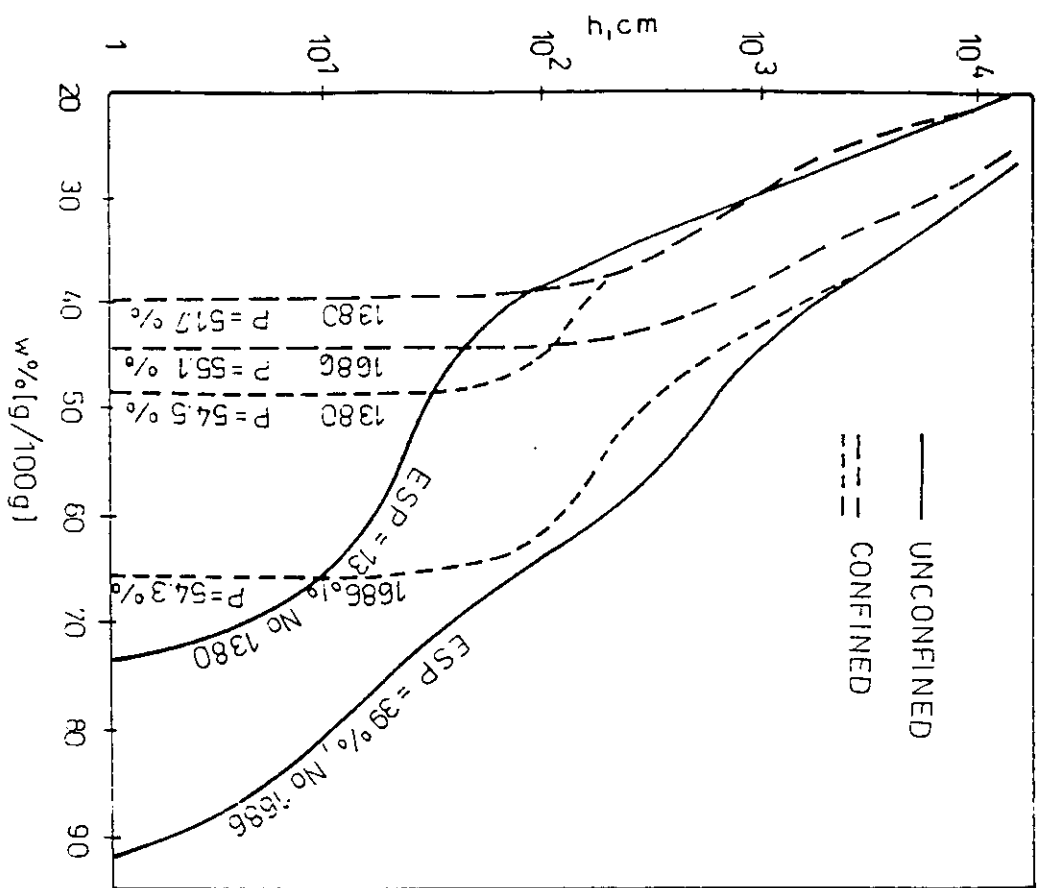
## 8. EVAPOTRANSPIRATION

---

**SH**  M. Kutilek & D.R. Nielsen: SOIL HYDROLOGY, Catena, 1994

---

1. Evaporation from bare field soil, **SH**, p. 190-193.
2. Physical interpretation of transpiration, **SH**, p. 195-201.
  - 2.1. Potential and actual transpiration, **SH**, p. 201-204.
  - 2.2. Wilting point, **SH**, p. 205-206. In saline and alkali soils, see Figs. 8.1. and 8.2.
3. Evapotranspiration, **SH**, p. 193-195
  - 3.1. Potential evapotranspiration, **SH**, p. 206-209.
  - 3.2. Structure of potential evapotranspiration, **SH**, p. 209-212.
  - 3.3. Actual evapotranspiration, **SH**, p. 212-217.



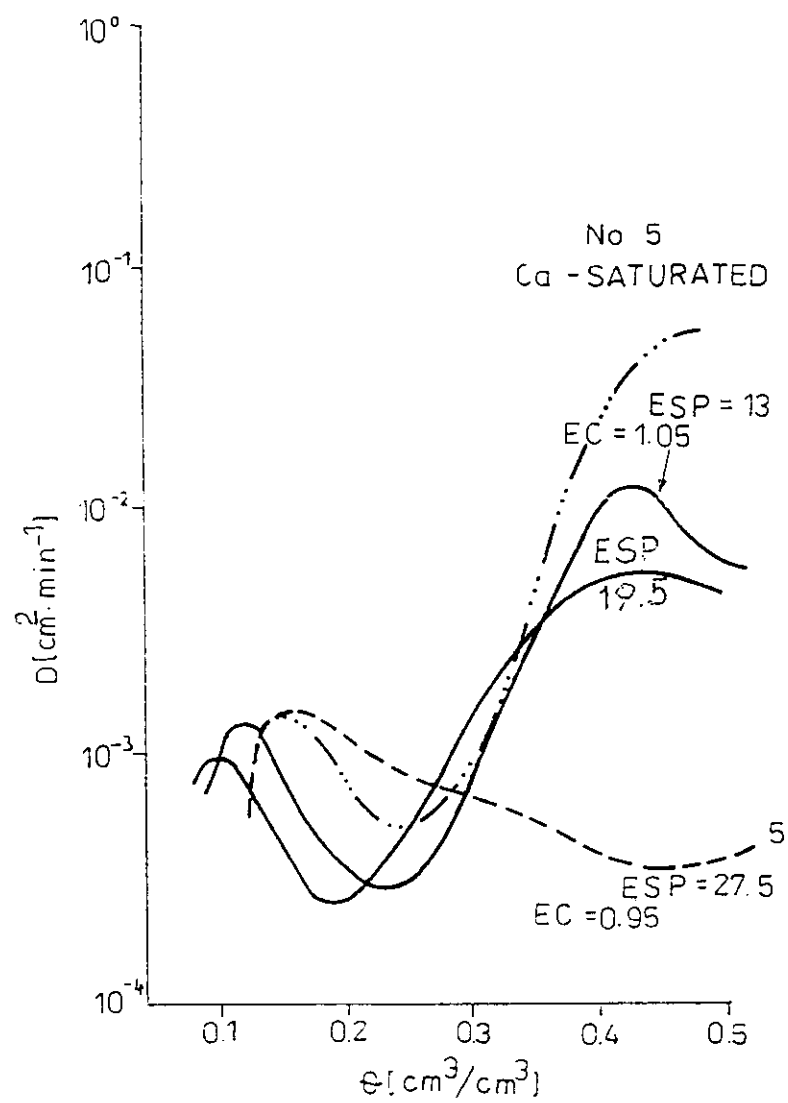


FIG. 8.2

## 2. WHY SCALING RE & RE+S IN EVAPOTRANSPIRATION ?

Two types of heterogeneities:

1. Heterogeneity of the soil,
2. Heterogeneity of the boundary condition on SAB

For heterogeneous boundary condition we solve:

(1) Space and time structure of  $t_r$  when potential evapotranspiration  $E_{TP}$  is reduced to  $E_{TA}$

$E_{TPi}$  ( $=q_{oi}$ ) at locations  $i$  are space-variable due to local climate and microclimate.

Space variability of  $t_{ri}$  can be estimated from scaled  $T^*$ , once  $t_r$  is known at one pedon-scale location with defined soil hydraulic functions.

(2) Space structure of soil water distribution with the depth  $\theta(z)_i$  when  $\theta(z)$  was measured on one vertical (pedon scale) and  $q_{oi}$  is known.

(3) For a set of measured  $\theta(z)_i$ , the space structure of fluxes  $q_{oi} = E_{TAi}$  on SAB is estimated.

(4) Hydraulic parameters of the soil-root system are not identical with independently measured soil parameters where roots are missing. If  $\theta(z)$  in soil with vegetation is measured together with  $q_o$ , we estimate "substitute hydraulic functions" of the soil-root zone applying the scaled RE.

The principle of the method is the transformation of the RE to the invariant form with regard to the variable flux on the boundary.



### 3. INVARIANT RE TO A VARIATION OF BC

Kutílek, M., K.Zayani, R.Haverkamp, J.Y. Parlange, G.Vachaud. 1991. *Scaling of the Richards equation under invariant flux boundary conditions*. Water Resour.Res. 27:2181-2185.

Hydraulic characteristics of the soil:

Soil water diffusivity  $D$  [ $L^2 T^{-1}$ ]

$$D(\theta) = D_o(\theta - \theta_r)^g \quad (1)$$

$\theta$  - soil water content,

$\theta_r$  - residual soil water content

Retention curve with pressure head  $h$  [L]

$$h(\theta) = -p(\theta - \theta_r)^{-u} \quad (2)$$

Unsaturated hydraulic conductivity  $K$  [ $L T^{-1}$ ]

$$K(\theta) = K_o(\theta - \theta_r)^v \quad (3)$$

$D_o, K_o, g, p, u, v$  - fitting parameters

Scaled variables:

$$t = q_o^\alpha T^*, \quad z = q_o^\beta Z^*, \quad \theta - \theta_r = q_o^\gamma \theta^* \quad (4)$$

$\alpha, \beta, \gamma$  - scaling factors

Scaled hydraulic functions:

$$D(\theta) = q_o^{g\gamma} D^*(\theta^*) \quad h(\theta) = q_o^{-u\gamma} h^*(\theta^*)$$

$$K(\theta) = q_o^{v\gamma} K^*(\theta^*) \quad (5)$$

Substitution of (4) and (5) into RE:

$$q_o^{\gamma-\alpha} \frac{\partial \theta^*}{\partial T^*} = q_o^{g\gamma + \gamma - 2\beta} \frac{\partial}{\partial Z^*} \left[ D^*(\theta^*) \frac{\partial \theta^*}{\partial Z^*} \right] + q_o^{v\gamma - \beta} \frac{\partial K^*(\theta^*)}{\partial Z^*} \quad (6)$$

In order to get (6) invariant to  $q_o$

$$\gamma - \alpha = v\gamma - \beta \quad \gamma - \alpha = (g + 1)\gamma - 2\beta \quad (6a)$$

Scaled BC:

$$T^* \geq 0, \quad Z^* = 0$$

$$q_o = q_o^{g\gamma + \gamma - \beta} D^*(\theta^*) \frac{\partial \theta^*}{\partial Z^*} - q_o^{v\gamma} K^*(\theta^*) \quad (7)$$

$$\text{For invariancy: } 1 = (g + 1)\gamma - \beta \text{ and } 1 = v\gamma \quad (7a)$$

Since  $D(\theta) = K(\theta)dh/d\theta$

$$q_o^{g\gamma} D^*(\theta^*) = q_o^{v\gamma - u\gamma - \gamma} K^*(\theta^*) \frac{dh^*}{d\theta^*} \quad (8)$$

$$\text{For invariancy: } g\gamma = v\gamma - u\gamma - \gamma$$

$$v = g + u + 1 \quad (8a)$$

SCALING FACTORS from (6a), (7a):

$$\alpha = \frac{-2u - g}{v}, \quad \beta = \frac{-u}{v}, \quad \gamma = \frac{1}{v} \quad (9)$$

Scaled RE invariant to the top BC

$$\frac{\partial \theta^*}{\partial T^*} = \frac{\partial}{\partial Z^*} \left[ D^*(\theta^*) \frac{\partial \theta^*}{\partial Z^*} \right] + \frac{\partial K^*(\theta^*)}{\partial Z^*}$$

SCALING OF RE + S

For approximations:  $\partial T_R / \partial t = 0$  and  $T_R \sim q_o$   
(dense vegetation), scaling factors are  
expressed by (9), too.

Analogically for SOIL WATER STORAGE  $W = \int_0^Z \theta \, dz$   
 $\partial W / \partial t = -K(W) \partial H / \partial z \quad q_o = \partial W / \partial t$

Nielsen, D.R., M.Kutílek, M.B.Parlange. 1996.

Surface soil water content regimes: opportunities  
in soil science. J.Hydrol. 184:35-55